Analysis of MIMO Relay Chains

David Manning

A thesis submitted in fulfillment
of the requirements for the degree of

Masters

in

Electrical and Electronic Engineering

University of Canterbury
Christchurch, New Zealand

September 2010

Abstract

This thesis is split into two parts: first a statistical analysis of multi-hop MIMO relay networks, followed by a simulation of the perfomance of a P25 SISO multi-hop relay network. The basis of the MIMO section is the developement of an end to end statistical model of the multiple relay channel. This end to end model simplifies the statistics involved, making the analysis of systems with large numbers of relays and antennas more practical. A partial system model is obtained. This is exact for a multiple input single output network and can be used to describe the received signal at a single antenna in a multiple output system. We go on to look at the relationship between end to end system parameters and the paramters of individual inter-relay channels. The SISO section contains a characterisation of BER for P25 relay chains. The effect of the SNR at each relay node, the nature of the channel and the number of relay hops on the BER is determined. Furthermore, the performance trends are compared for a range of common relaying protocols, including amplify and forward and two types of decode and forward.

Acknowledgements

The author of this work would like to thank Peter Smith, Clive Horn and Jim Cavers for their continued support in the pursuit of this research. Appreciation is also owed to Jeremy Reece for his efforts in obtaining funding to support this work.

Contents

List of Figures

List of Tables

Abbreviations

AF - Amplify and forward

BER - Bit error rate

BPSK - Binary phase shift keying

CSI - Channel state information

CB - Citizen Band

DecR - Decode and regenerate

DetR - Detect and regenerate

FIR - Finite impulse response

GEV - Generalised extreme value distribution

ISI - Inter-symbol interference

LOS - Line of sight

MAC - Media access control

MIMO - Multiple input multiple output

SISO - Single input single output

NSR_{eq} - Equivalent end to end noise to signal ratio

QAM - Quadrature amplitude modulation

PF - Phase forward

SNR - Signal to noise ratio

SNR_{eq} - Equivalent end to end signal to noise ratio

SVD - Singular value decomposition

TCM - Trellis coded modulation

ZMCSCG - Zero mean circularly symmetric complex Gaussian

Chapter 1

Introduction

When building a communications network, an important consideration is that of topology [1]. That is, which parts of the network will interact. Two obvious arrangements are centrally routed networks and networks using direct connections. In a centrally routed network terminal nodes communicate via a single interchange node. In a network using direct connections terminal nodes communicate directly with each other. In practice most networks will fall somewhere between these two extremes. For example, in a cell phone network [2] users communicate via a single base station within a given area or cell. Users in different cells communicate with their respective base stations which will transfer the information between them. The internet works in a similar manner, albeit with a larger hierarchy. Here a user will connect to an internet service provider, which in turn may connect to a nationwide exchange and then an intercontinental router. On the other end of the spectrum, citizen band (CB) radio [3] is an example of a network utilizing direct connections between users. As may be apparent from the above examples, different topologies are more appropriate for different types of network.

A centrally routed network is more suited to dealing with a high user density and can help centralize the cost of establishing a network, that is the capital investment is primarily in the base stations as opposed to being split evenly between all radio nodes. In this context, high user density refers to a situation where it can be expected that a large proportion of the available bandwidth of the network will be

required simultaneously, by a large number of users. This would typically require bandwidth to be allocated to users dynamically and reassigned with a low latency [2]. A centrally routed network simplifies this task as, if all communications are transferred via one node, then the allocation of bandwidth can be managed by this node alone. This task is referred to as media access control (MAC) [1]. The fact that MAC can be dealt with solely in the central node allows the majority of the complexity and therefore the cost of network hardware to reside in this node. The result of this is the opportunity to produce low cost terminal nodes which, combined with the centrally routed system's suitability to high user densities, means that a network of this style has an easily scalable number of users. In a network with direct routing all the terminals need to be capable of any MAC the network implements. This limits the practical user density of a network of this type to the complexity that can be included in the terminal nodes. As such the investment per user in the network is higher than a centrally routed scheme but as no additional infrastructure is required the network can be ad hoc in nature. Systems providing scope for direct communications between users typically provide more geographical scalability than centrally routed networks while providing less scope for high user densities. This is not fundamentally the case but rather arises from the typical implementation of these network types.

Current radio products are predominantly of two types, privately owned radio terminals utilizing direct communications on public frequencies and commercial radio networks [4]. The commercial networks are typically centrally routed, with fixed high power central nodes. This is the context for the work in this thesis. The key question is whether some of the flexibility advantages of direct point to point communications can be utilized in radio networks built around expensive fixed base stations. In particular this work looks at using the concept of relays [5] to provide this flexibility. A relay in this context is considered to be a network node which immediately retransmits what it receives, possibly with some intermediary processing. The purpose of the relay node is to extend the range over which other nodes in the network can communicate, or reduce the transmission power required by the

nodes to communicate within a given area. It should also remain as transparent as possible [6]. By transparent we mean that communication between users should be equivalent to the case where they are in a range where the relay is not needed. That is the performance and operation of the system should be virtualy the same as in the case where the relay is not used.

The concept of using relays for communication is not new, in fact it could be considered as the basis of some of the earliest communication networks. From semaphore chains to smoke signals to wolf howls, relaying signals provided a simple means of long distance communication. Modern examples of relays augmenting a larger network include; relays for cell phone signals located inside large buildings, which have poor reception from the nearest base station. This relay may be connected to an aerial external to the building, where the signal to the rest of the network is stronger. A very crude relay is the leaky feeder [7], a length of coaxial cable which runs along the length of a tunnel and is connected to an aerial outside the tunnel. This allows radio signals to propagate inside the tunnel. Here we consider the possibility of a more extensive augmentation of existing networks with the relay concept, or even stand alone relay based networks. These could be of use in areas of low user density, where the full sophistication of a base station is not required. The key requirement of a relay for this purpose is to be of low cost, so as to provide a useful alternative to installing a base station. Another desirable property is to possess a low power requirement. This will allow the possibility of being battery powered and portable. A product of this nature would provide a low cost, easily scalable and portable network infrastructure. Situations where this could be of commercial value include:

- Areas with very low user density, such as rural areas, where little MAC is required. Here the sophistication of a typical base station is unnecessary so a relay system could provide the same coverage at a much lower cost.

- Temporary networks to provide coverage in remote areas, such as that required by emergency services. Here the potential portability of relays could be utilized to drop them into a location, or mount them in a vehicle, allowing coverage to

be relocated as required.

- Extension of existing networks into areas of low user density. These areas may not prove economic to cover with a base station, but could be serviced by relaying signals to an existing base station adjacent to the area [8]. This is outlined in Fig. 1.1.

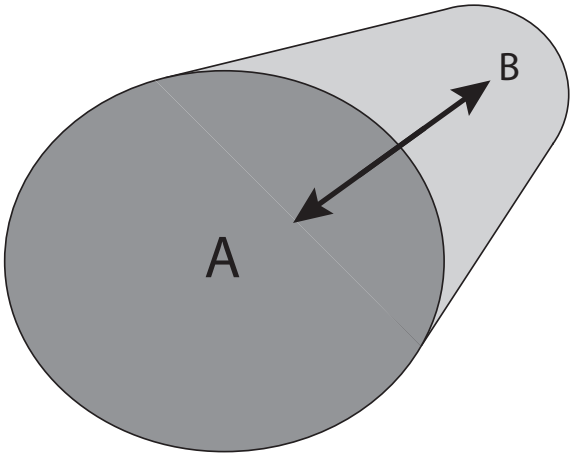

Figure 1.1: Coverage for area B with low user density is provided by relaying signals between B and the high density area A

- Extending or establishing new networks in heavily shadowed areas, such as valleys, tunnels, buildings etc. Shadowing [9] refers to the situation where large objects block the path of radio propagation, hills and buildings would be typical examples. These objects drastically weaken the signal in their path. In areas with heavy shadowing the use of single high power transmitters is inefficient, as most of the transmit power is not received. A solution is to use a sequence of lower power transmitters to relay the signal around the shadowing objects. Figure 1.2 is an example of this scenario.

Of course an obvious question relating to a relay system of this nature is: how big can a network based on this concept become? There are two ways to increase the network coverage, increasing transmit power and adding more relying nodes [5]. Increasing transmit power removes some of the advantages of the relay concept so is not necessarily desirable. Hence, network expansion would ideally be performed via increasing the number of relays used. The issue then becomes how many relays can

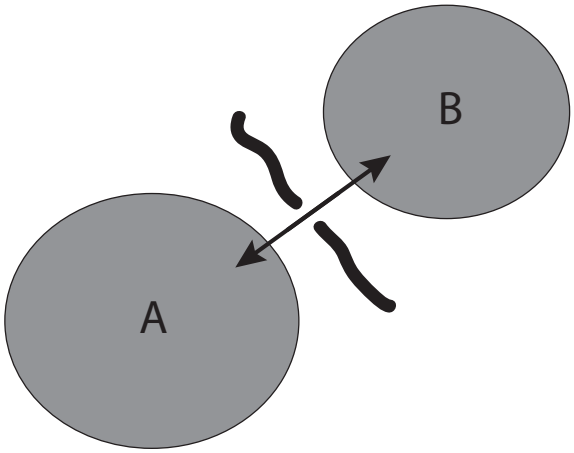

Figure 1.2: A connection between areas A and B is provided by a relay chain through the shadowing object between them

a signal pass through while retaining an acceptable number of errors. Anyone who has played the game Chinese whispers will identify the problem that if each relay has the potential to introduce errors into communication, the combination of multiple relays increases the probability of errors. To allow the use of chains of relays it is important to investigate what can be done within the relay node to mitigate this problem and to establish what kinds of conditions these relay networks can operate in. This work focuses on the effect of increasing the number of relay nodes in the communication path, with a variety of relay types and radio environments.

Also under consideration is the use of MIMO transmission with relay networks [10]. MIMO stands for multiple input multiple output and refers to the use of antenna arrays for both transmission and reception of information. For example a single transmitter could use multiple antennas to transmit to a receiver with multiple antennas. Alternatively a set of transmitters with single antennas could transmit cooperatively to a set of receivers with single antennas. The advantage of multiple antennas is that it provides spatial diversity. This effect can provide more reliable transmission or can be used to increase the potential capacity of a wireless channel. Due to local scattering effects the strength of a radio signal at separate antennas even if they are located close to each other can vary drastically. Hence the use of multiple antennas gives a higher probability of receiving a strong signal at one of the antennas. Thus, if the same information is transmitted on each antenna the error probability

of the channel drops. Furthermore, if the channel properties between each antenna pair can be tracked by the receiver it is possible to transmit independent information on each antenna. Antenna arrays at a single node provide this spatial diversity on a scale of the order of the wavelength of the signal, providing robustness to local scattering effects. In contrast an array of separate nodes provide a similar effect on a larger spatial scale. This arrangement can provide redundancy against shadowing as well as local scattering. The downside to this arrangement is that the geographically separated nodes need a reliable connection with low delays in order to communicate cooperatively. This would normally involve a wired connection.

The current knowledge of relay chains can be split into two broad areas: relays using MIMO techniques and those using traditional single antenna systems, referred to as single input single output (SISO) systems. For MIMO systems, the results available relating to relay performance are limited but, as with other areas of MIMO communications, it is an active area of research [11]. Furthermore, multi-hop relaying using MIMO techniques is in its infancy in terms of performance analysis. Some results for capacities in relation to numbers of relay nodes and antennas are available [12, 13]. Optimal relaying techniques and coding structures are developed in [14] assuming full channel state information (CSI) at each relay. An asymptotic performance analysis is presented for this system in [14].

Research into SISO communications is more developed, as would be expected due to its much longer history. It is important to note that these single antenna systems can still benefit from spatial diversity when multiple relay nodes are used for signal transmission. As multiple nodes are transmitting the same information in a multi-hop relay system, a receiver capable of combining signals from all transmission sources can benefit from this diversity. General results for multi-hop relaying have still proved difficult to obtain though, an overview of available results is given in [15]. The system performance is dependent on the type of relay processing performed which complicates a summary of the available knowledge. Introducing the concepts of analogue and digital relaying make this summary easier. Here, an analogue relay is one that amplifies the received signal without performing any other

processing, while a digital relay performs some degree of demodulation and decoding before regenerating and retransmitting the signal. With an arbitrary hop length [16] and [17] give upper bounds on errors for digital relays and analogue relays using a specific amplification factor. [16] contains an analysis for systems using the diversity offered by multiple relays and [17] performs a similar analysis for systems without this diversity. An approximate expression for error rates is developed in [18] which applies to analogue relays of arbitrary hop length and includes diversity. The instantaneous end to end SNR is found in [19] for multi-hop analogue relaying with diversity. The system error rate is found in [20] for digital relays.

1.1 Goals

The available results for multi-hop MIMO relay systems are limited as a result of the highly complex statistics of the resulting propagation channel. Currently, the systems are modeled via a combination of the existing models for the channel between two radio nodes. The result is a model where the degrees of freedom are proportional to the number of relay nodes and the square of the antenna numbers. The motivation of the work presented in Chap. 3 is to develop a model which describes the statistics of the end to end channel directly, ideally massively reducing the degrees of freedom of the model. This may lead to an easier analysis of the performance of the system. For example, error rates and end to end signal to noise ratios for multi-hop MIMO relay channels are not currently available. An understanding of the statistics of the complete channel may lead to these expressions. Parallel to this investigation, Chapter 4 looks at performance metrics of a SISO system using the P25 protocol.

1.2 Contributions

The thesis makes contributions in both areas of interest, namely in the analysis of MIMO relay channels and in the evaluation of various SISO relay implementations. Firstly a partial end to end channel model is developed in Chap. 3 for analogue

relays. Using this model we go on to develop expressions for moments of the elements of the end to end transfer function, probability densities for the single relay case and expressions for the end to end signal to noise ratios in the system. We go on to look at the effects the relay amplification and a capacity analysis based on the eigenvalues of the transfer matrix.

The analysis of the SISO system, while providing results for the specific modulation scheme outlined in the P25 specification, also addresses some general questions arising in the literature. The majority of work done in relation to multi-hop relays focuses on flat fading channels. The SISO simulations presented in Chapter 4 include the error rate trends for multipath channels with a variety of common relaying protocols. This introduces the problem of inter-symbol interference (ISI), which proves to be significant and in some cases the dominant cause of errors.

1.3 Thesis Organization

Chapter 2 outlines the existing system models based on single hop transmission and shows how these can be cascaded to describe a multi-hop system. The description of the model is split into that relevant to MIMO communications, followed by that applicable to SISO communications. The description of the system model is further split into four components, the source signals, the propagation channel, the relaying protocol and the noise components. These are all described separately for MIMO and SISO communications.

Chapter 3 develops the statistics of the end to end signal model and presents the results relevant to performance that can be obtained from this model. A look at the dependence structure in the end to end transfer function of the channel is given is presented first, the raw moments of elements of the system model follow. End to end signal to noise ratio distributions are presented next including their moments. The effects of the linear amplifiers are considered. The penultimate section contains an empirical analysis of the eigenvalues with an explanation of how these can be related to capacity. Finally we look at channel model approximations.

Chapter 4 presents the results of the simulations of a P25 SISO multi-hop relay

channel. The simulated results are presented in such a way as to isolate the effects of individual degrading channel properties. First we demonstrate the effect of slow fading on the communication scheme across a range of relaying protocols and identify the cause for the discrepancies in the relay protocols. The results of fast fading are covered next. Both these sections look at relay protocols ability to mitigate the effects of frequency selective channels. The complete system model is considered next. This section looks at conditions in which a desired error rate can be maintained and is intended to aid system design. The final section looks at requirements for maintaining block error rates using error correcting codes.

Finally, Chapter 5 presents some conclusions and directions for future work.

Chapter 2

System Model

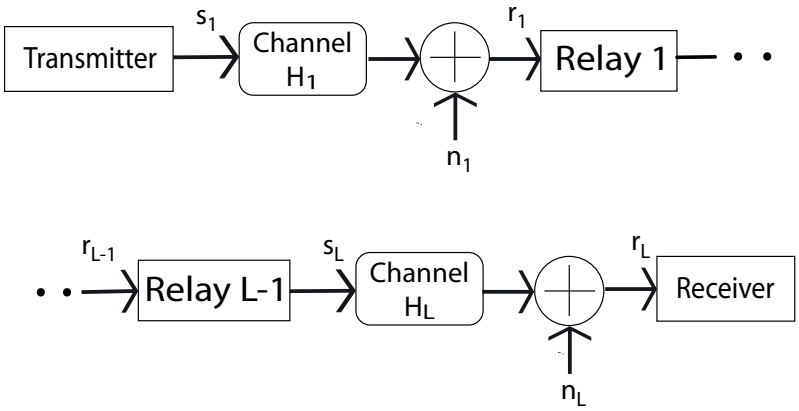

Figure 2.1: System diagram for a relay chain with L hops

The work in Chaps. 3 and 4 is split into an analytical component involving MIMO techniques and simulation work based on SISO transmission. As the nature of many system components is different for these two scenarios, the system model for each part will be described separately. Given that a SISO communication system is a special case of the more general MIMO model, the MIMO section will be described first in, Sec. 2.3, with the SISO specific model following in Sec. 2.4. As a preliminary, some notation, performance metrics and system parameters will be defined. Despite the differences between the two scenarios the common structure of a typical L-hop relay chain can be identified in Fig. 2.1.

To describe the general system in Fig. 2.1 we need to define the signal vectors $\mathbf{s}_1, \mathbf{s}_2, \ldots, \mathbf{s}_L$, $\mathbf{r}_1, \mathbf{r}_2, \ldots, \mathbf{r}_L$ and noise vectors $\mathbf{n}_1, \mathbf{n}_2, \ldots, \mathbf{n}_L$. The originally trans-

mitted signal, $\mathbf{s}_1$, passes through the first channel, which has transfer function $\mathbf{H}_1$. This is received, along with additive Gaussian noise, $\mathbf{n}_1$, at the first relay. The received signal, $\mathbf{r}_1$, is given as $\mathbf{r}_1 = \mathbf{H}_1 \bigotimes \mathbf{s}_1 + \mathbf{n}_1$, with $\bigotimes$ being the convolution operator. The dimension of the vector $\mathbf{s}_1$ is given by the number of transmit antennas which in this work will be referred to as N_1. The dimension of $\mathbf{r_1}$ and $\mathbf{n}_1$ is the number of receive antennas, denoted by M_1. The received signal, $\mathbf{r}_1$, is processed by the relay, producing the signal transmitted by the first relay, referred to as $\mathbf{s}_2$. The relationship between $\mathbf{r}_1$ and $\mathbf{s}_2$ depends on the type of relay protocol being employed. $\mathbf{r}_2$ is then $\mathbf{H}_2 \bigotimes \mathbf{s}_2 + \mathbf{n}_2$ and $\mathbf{r}_L = \mathbf{H}_L \bigotimes \mathbf{s}_L + \mathbf{n}_L$. The number of receive antennas at the l^{th} relay and the dimension of the vectors $\mathbf{n}_l$ and $\mathbf{r}_l$ is denoted M_l. The number of transmit antennas at the l^{th} relay and the dimension of $\mathbf{s}_{l+1}$ is denoted N_l. Given these definitions, the transfer function between the l^{th} and $(l-1)^{th}$ relays has N_{l-1} inputs and M_L outputs. In general these equations require a convolution of the signal with the channel transfer function. If this transfer function is an impulse, then this reduces to a multiplication. In practice, this represents a channel which does not spread a signal in time. As an approximation to a physical system this is valid provided the difference in propagation delay across all possible paths is less than the symbol period. Channels of this type are referred to as flat fading channels, as the attenuation of the channel is independent of frequency. For the MIMO system in Chap. 3 a channel model of this form is used. This chapter looks to provide an expression for the end to end transfer function of the relay link, that is to specify the signal at the final receiver directly in terms of the originally transmitted signal. This will be an equation of the form $\mathbf{r} = \mathbf{H}_{eq} \bigotimes \mathbf{s}_1 + \mathbf{n}_{eq}$, with $\mathbf{H}_{eq}$ being the equivalent transfer function between the transmitted signal and the information carrying component of the received signal. The noise terms, $\mathbf{n}_{eq}$, represents the cumulative noise received through the relay link. It is now left to define the channel transfer functions $\{\mathbf{H}_1, \mathbf{H}_2, \dots\}$, the nature of the transmitted signal $\mathbf{s}_1$ and the noises $\{\mathbf{n}_1, \mathbf{n}_2, \dots\}$ in terms of the relaying techniques used.

2.1 Notation

Matrices

- Matrices are represented by bold capital letters such as $\mathbf{H}$.
- H_{mn} refers to the element from the m^{th} row of the n^{th} column of $\mathbf{H}$.
- $\mathbf{H}_m$ refers to the m^{th} row of $\mathbf{H}$.
- $\mathbf{H}_n$ refers to the n^{th} column of $\mathbf{H}$.
- Some equations will use specific indices, such as $\mathbf{H}_1$, to denote either the first column or row of $\mathbf{H}$. Whether this refers to the row or column will be apparent from the context.
- Equations will also use notation such as $\mathbf{H}_l$ to denote a single matrix from a set of matrices $\mathbf{H}_l, l \in \{1, 2, \ldots, L\}$. Once again, the fact that this is a full matrix rather than a row or column vector will be apparent by context. To refer to an element of such a matrix the notation $(H_l)_{mn}$ is used to represent the element from the m^{th} row of the n^{th} column of $\mathbf{H}_l$. Similarly the m^{th} row of $\mathbf{H}_l$ is denoted $(\mathbf{H}_l)_m$ and n^{th} column, $(\mathbf{H}_l)_n$.

Vectors

- Vectors are represented by bold lower case letters such as $\mathbf{s}$.
- s_m refers to the m^{th} element of $\mathbf{s}$.
- $\mathbf{s}_k$ refers to the k^{th} vector in the set $\mathbf{s}_k, k \in \{1, 2, \ldots, L\}$, s_{km} refers to the m^{th} element of this vector.

Products

Empty product expressions are considered to be equal to one. For example, $\prod_{l=L+1}^{L} \mathbf{H}_l = 1$.

Random Variables

The system models make considerable use of zero mean circularly symmetric

complex Gaussian variables (ZMCSCG), which are of the form $z_1 + jz_2$ where z_1, z_2 are i.i.d real zero mean Gaussian variables. We also define $\mathbb{C}N(0,1)$ to be the distribution of a ZMCSCG variable with unit variance.

Complex Variables

Complex conjugates and Hermitian transposes will be denoted by the symbol †. That is, a scalar x has complex conjugate $x^\dagger$, a vector, $\mathbf{s}$, has Hermitian transpose $\mathbf{s}^\dagger$ and a matrix, $\mathbf{H}$, has Hermitian transpose $\mathbf{H}^\dagger$.

2.2 Metrics and System Parameters

When quantifying the performance of communication systems, a variety of metrics can be used. The metrics used in this work are:

Capacity This is a measure based on information theory giving an upper bound on the rate of the communication system that can be maintained while retaining no transmission errors.

Bit Error Rate (BER) This metric gives the number of bit discrepancies between the transmitted and received message as a fraction of the total number of bits contained in the message. The ratio given is normally an average with the message size tending to infinity as the number of bit errors for any given message will vary.

Block Error Rate (BLER) Similar to BER the BLER is often applied to transmission schemes that send data in discrete, finite blocks. Here the ratio of blocks containing one or more errors to the total number of blocks transmitted is given.

Fundamentally, all performance measures of a communication system are dependent on the ratio of the received signal power to the received noise power. Let r be the scalar received signal at a single antenna and n be the scalar noise at the same single receive antenna. The signal to noise ratio (SNR) is defined as $\frac{E[|r|^2]}{E[|n|^2]}$ giving the average received signal to noise power ratio.

2.3 Multi-hop MIMO Relayed Communications

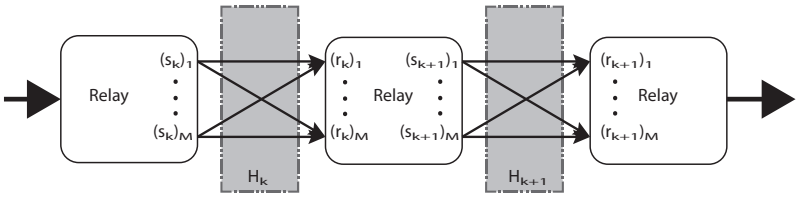

Figure 2.2: System diagram for a partial section of a MIMO multi-hop relay link

For the MIMO system we will focus on flat fading channels. As the transfer function of this channel is an impulse, the effect of the channel in the system model reduces to a multiplication. A partial multi-hop MIMO link is shown in Fig. 2.2. We can define the received signal at the first relay as $\mathbf{r}_1 = \mathbf{H}_1\mathbf{s}_1 + \mathbf{n}_1$. This received signal is then processed by the relay to give $\mathbf{s}_2$, the signal transmitted by the first relay. In general the received signal at the l^{th} relay is given by $\mathbf{r}_l = \mathbf{H}_l\mathbf{s}_l + \mathbf{n}_l$.

2.3.1 Channel Model

For the MIMO relays the standard Rayleigh scattering model of wireless propagation is used. Here the gain between any transmit/receive antenna pair is given by a variable distributed as a ZMCSCG variable. The model represents propagation scenarios in which there is no line of sight (LOS) path present and it assumes a large degree of scattering of the signal at the receiver. It can be shown in this situation that the attenuation between an antenna pair is Rayleigh distributed [9]. Hence the PDF of the channel attenuation is given in [21] Chap. 18 Sec. 10.2 as

$$p(x) = \frac{x}{\sigma^2}\exp\left(\frac{-x^2}{2\sigma^2}\right), x \geq 0$$

where σ is the distribution scale parameter, which in this case specifies the average channel attenuation. The phase shift of the channel is uniformly distributed between $-\pi$ and π.

In a MIMO system [22] the gains between each antenna pair can be represented in a matrix structure such as

$$\mathbf{H} = \begin{bmatrix} H_{1,1} & \cdots & H_{1,N} \\ \vdots & \ddots & \vdots \\ H_{M,1} & \cdots & H_{M,N} \end{bmatrix},$$

for a MIMO system with N transmit antennas and M receive antennas. Such a system will be referred to as $M \times N$ MIMO. Each element, $H_{m,n}$, in $\mathbf{H}$ is distributed as an i.i.d ZMCSCG variable. $\mathbf{H}$ is referred to as the channel matrix. If $\mathbf{s}$ is an $N \times 1$ vector representing the signals at the N transmitters then the signals received at the M receivers are given as $\mathbf{r} = \mathbf{Hs}$. In the presence of noise this becomes $\mathbf{r} = \mathbf{Hs} + \mathbf{n}$ where $\mathbf{n}$ is an $M \times 1$ vector of i.i.d complex Gaussian variables.

The Rayleigh model represents local scattering of the signal at the receiver. To account for shadowing between transmit and receive antennas an additional log-normal scaling parameter is normally used, while free space path loss is represented by another parameter. The work in Chaps. 3 and 4 does not focus on a specific physical system so a distance or antenna coefficient for the free space path loss cannot be specified. Shadowing is also a constant scaling parameter for a given inter node channel. Hence we remove both of these components from our channel model and instead we simply specify the SNR at the receiver. This is justified based on the fact that for a physical radio link the degree of shadowing experienced will remain relatively constant over the period of transmission. Hence from the point of view of system design it is just as useful to evaluate the links performance at a given average SNR.

Time Varying Channels

The channel model described here is based on the idea of a large number of scattered signal paths combining randomly at the receiver to produce the received signal. This suggests that the received signal will vary in space. Hence a moving receiver will experience a time dependent channel. Similarly, if an object around the receiver that is affecting the scattered signal is moving, then even a stationary receiver will experience a channel that varies over time [9]. The effect is the same if the transmitter is moving in space so the relative motion between transmitter, receiver

and objects in the propagation environment dictates the extent of this effect. For the purpose of analysis in wireless communications, the rate of change of the channel is broken into two categories, these being fast and slow fading channels. In a slow fading channel the rate of change of the channel is considered to be of an order such that over a symbol period of the modulation scheme the channel can be considered to be static. In this situation the performance of the communication scheme is not affected directly by the changing channel, but the average performance of the system will be dependent on how the channel properties change over time. In a fast fading environment the channel properties are assumed to change significantly within a symbol period and will potentially affect the demodulated signal.

We use a model of fast fading based on the Jakes Doppler spectrum [9]. With this model the change over time can be defined by an autocorrelation function $R(\tau) = J_0(2\pi f_d \tau)$ where J_0 is the zeroth-order Bessel function of the first kind, f_d is the maximum doppler shift and τ is the time between two channel instances. $R(\tau)$ is the autocorrelation function of an element of the channel matrix, $\mathbf{H}$. For the complex element, H_{mn}, the autocorrelation function is defined as $R(\tau) = E[(H_{mn})_t^{\dagger}(H_{mn})_{t+\tau}]$, where the subscript refers to the time at which H_{mn} is observed. The maximum doppler shift is defined as $f_d = \frac{v f_c}{c}$ where f_c is the carrier frequency and v is the relative velocity of the transmitter and receiver or the scattering objects. Figure 2.3 is a plot of the normalized auto correlation and gives a measure of the expected commonality between two instances of the channel with a separation in time given by $\frac{\tau}{f_d}$.

The effect of a time varying channel on the received signal depends on the type of modulation employed by the communication system. When using a constant envelope, non-coherent modulation such as DPSK the change in channel properties across adjacent symbols introduces errors in the received signal. When designing a system to operate in these conditions the autocorrelation function of the channel can be used to give an indication of acceptable symbol rates for a given error margin. It can be seen from Fig. 2.3 that the higher the symbol frequency the greater correlation between the channel conditions at a adjacent symbol times. With DPSK

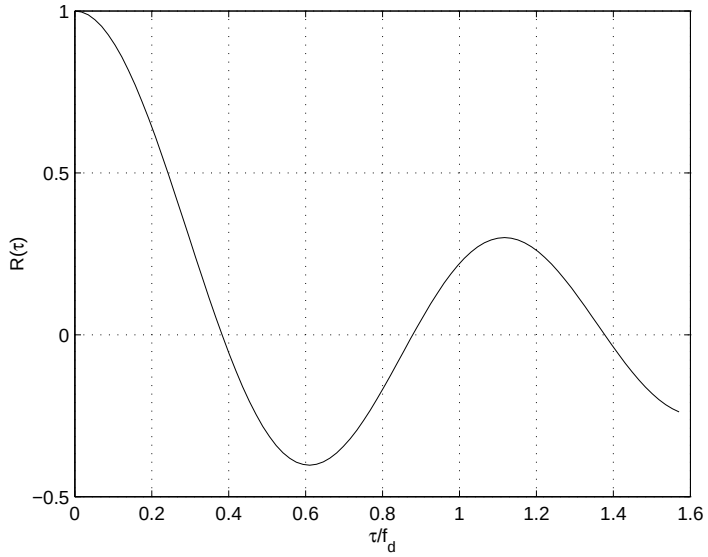

Figure 2.3: Fast fading autocorrelation function

modulation a change in the channel phase shift between sample times will introduce an error in the demodulated signal. Hence, a higher correlation between channel properties at adjacent sample times results in a lower error probability. Figure 2.3 also suggests that there is a lower limit to symbol frequency for a practical DPSK system giving by the first zero crossing of the channel autocorrelation function. At this point the channel properties are not reliably correlated between adjacent samples.

2.3.2 Source Signals

The source signals, $\mathbf{s_1}$, are $N_1 \times 1$ vectors drawn from a random sequence at a rate given by the sample frequency of the communication protocol. The samples drawn from the sequence are assumed to be uncorrelated. Furthermore $E[\mathbf{s}_1^\dagger \mathbf{s}_1]$ is assumed to be equal to one.

2.3.3 Relay Protocols

The types of relaying considered are split into two general categories. In the literature these are often referred to as linear relaying and decoded relaying [10] and

correspond to the use of analogue or digital relays respectively. In decoded relaying the message is estimated at each relay and regenerated. As a result, the end to end channel properties are not important and each hop in the relay link can be considered independently. The problem in evaluating the performance with decoded relaying becomes one of describing error propagation as decision errors from one relay will be transmitted to the next. Chapter 3 does not look at this issue and the analytical work focuses on linear relaying. Relays of this type retransmit the received signal with some form of linear transformation, α, hence the transmitted signal for relay one is given by $\mathbf{s}_2 = \alpha_1 \mathbf{r}_1$ where

$$\mathbf{s}_2 = \alpha_1(\mathbf{H}_1\mathbf{s}_1 + \mathbf{n}_1).$$

This pattern can be continued to give the signals throughout the relay chain. Let the received signal at the l^{th} relay be $\mathbf{r}_l$, the signal transmitted from the l^{th} relay be $\mathbf{s}_{l+1}$, the channel transfer function between the $(l-1)^{th}$ and l^{th} relays be $\mathbf{H}_l$ and the received noise at the l^{th} relay be $\mathbf{n}_l$. With these definitions

$$\begin{aligned} \mathbf{r}_l &= \mathbf{H}_l\mathbf{s}_l + \mathbf{n}_l, \\ \mathbf{s}_{l+1} &= \alpha_l\mathbf{r}_l, \\ \mathbf{s}_{l+1} &= \alpha_l(\mathbf{H}_l\mathbf{s}_l + \mathbf{n}_l). \end{aligned} \tag{2.1}$$

Expanding (2.1) recursively we can define the signal at the final receiver, $\mathbf{r}_L$, in terms of the signal at the original transmitter, $\mathbf{s}_1$, giving an end to end system equation. This is shown in Sec. 3.1.

The general form for α_l is an $M_l \times N_l$ complex matrix. This allows the possibility of the output at each antenna on the transmit side of the relay being a linear combination of the inputs at each antenna on the receive side. An important special case of this general form is a diagonal α_l matrix. Here, the signal received at each antenna is scaled to give the output at a transmit antenna. Hence there is no combining of signals, simply a scaling. A further simplification is the reduction of α_l to a scalar, where there is once again no combining of signals and only a simple scaling factor is used.

2.3.4 Noise

The system model includes additive Gaussian noise at each receive antenna. Complex Gaussian noise is assumed. Hence the noise, n, is given by $\sqrt{\frac{N_0}{2}}(n_r + jn_i)$ where n_r and n_i are i.i.d real Gaussian variables and $N_0/2$ is the power spectral density of the noise.

2.3.5 Signal Power

To provide a general model for the relay system it is desirable to normalize the signal powers in the system model. To achieve this the various parts of the system can be redefined as follows. Let the physical signal at the first relay be defined by

$$\tilde{\mathbf{s}}_2 = \tilde{\alpha}(\tilde{\mathbf{H}}_1\tilde{\mathbf{s}}_1 + \tilde{\mathbf{n}}_1). \tag{2.2}$$

We will write (2.2) in terms of a set of signals with unit power scaled by the power of the signals in the actual physical system.

$$\sqrt{P_{s_2}}\mathbf{s}_2 = \tilde{\alpha}(\sqrt{P_H}\mathbf{H}_1\sqrt{P_{s_1}}\mathbf{s}_1 + \sqrt{P_n}\hat{\mathbf{n}}_1) \tag{2.3}$$

Here, $\mathbf{H}_1$ is the normalized channel matrix where $E[|(\mathbf{H}_1)_{mn}|^2] = 1$, $\mathbf{s}_1$, $\mathbf{s}_2$ and $\hat{\mathbf{n}}_1$ are normalized transmit signals and noise vectors in the same fashion. $P_{s_2} = E[\tilde{\mathbf{s}}_2^\dagger\tilde{\mathbf{s}}_2], P_{s_1} = E[\tilde{\mathbf{s}}_1^\dagger\tilde{\mathbf{s}}_1], P_H = E[|(\tilde{\mathbf{H}}_1)_{mn}|^2], P_n = E[|\tilde{\mathbf{n}}_{1,m}|^2]$. Dividing (2.3) by $\sqrt{P_H P_{s_1}}$ we have

$$\frac{\sqrt{P_{s_2}}}{\sqrt{P_H P_{s_1}}}\mathbf{s}_2 = \tilde{\alpha}(\mathbf{H}_1\mathbf{s}_1 + \frac{\sqrt{P_n}}{\sqrt{P_H P_{s_1}}}\hat{\mathbf{n}}_1),$$

$$\mathbf{s}_2 = \frac{\sqrt{P_H P_{s_1}}}{\sqrt{P_{s_2}}}\tilde{\alpha}(\mathbf{H}_1\mathbf{s}_1 + \frac{\sqrt{P_n}}{\sqrt{P_H P_{s_1}}}\hat{\mathbf{n}}_1).$$

If we then define a normalized amplification factor, α, as

$$\alpha = \frac{\sqrt{P_H P_{s_1}}}{\sqrt{P_{s_2}}}\tilde{\alpha},$$

and another noise term, $\mathbf{n}_1$, where

$$E[\mathbf{n}_1\mathbf{n}_1^\dagger] = \frac{P_n}{P_H P_{s_1}}\mathbf{I},$$

then we have the normalized system model

$$\mathbf{s}_2 = \alpha(\mathbf{H}_1\mathbf{s}_1 + \mathbf{n}_1).$$

Since α is still an arbitrary scaling variable we can represent the various signal powers in the system by the variance of $\mathbf{n}_1$ alone. Furthermore, $\frac{P_n}{P_H P_{s_1}}$ is equal to the inverse of the signal to noise ratio, $\frac{1}{SNR}$, and the model can be defined directly by this parameter. Hence in system modeling it is sufficient to define the SNR and use unit power channels and signals.

2.4 Multi-hop SISO Relayed Communications

When using SISO communications the system model becomes scalar, but here we allow the possibility of the radio channel spreading the signal in time. This requires a convolution in the system equations. The received signal at the first relay, r_1, is given by $h_1 \bigotimes s_1 + n_1$. In SISO systems the possibility of non linear relay processing is considered, so an end to end system equation is not necessarily obtainable. The signals at the l^{th} relay can still be defined as r_l, s_{l+1} and n_l with the transfer function between the l^{th} and $(l-1)^{th}$ relay being h_l. The received signals are defined by

$$r_l = h_l \bigotimes s_l + n_l.$$

The relationship between r_l and s_{l+1} depends on the relay protocol employed and is covered in Sec. 2.4.5.

2.4.1 Channel Model

Here we use the flat Rayleigh channel as a reference to which the more complex propagation models can be compared. In the results presented, the flat Rayleigh channel shows the effects of the fading channel in isolation which allows the effect of

the other channel distortions to be assessed by comparison. The other channel models used here are extensions of the Rayleigh propagation concept, which allow the inclusion of phenomena such as ISI and the time varying channel causing distortion of the demodulated signal. These extended models will be described here.

While the Rayleigh model accounts for the local scattering of the received signal it does not allow for a LOS signal from the transmitter. The model can be extended to allow a non zero mean amplitude representing the presence of a LOS path. This is referred to as a Rician channel [9], where the channel attenuation distribution is defined by the PDF [21] Chap. 18 Sec. 10.7

$$p(x) = \frac{x}{\sigma^2} \exp\left(\frac{-(x^2+\mu^2)}{2\sigma^2}\right) I_0\left(\frac{x\mu}{\sigma^2}\right), \; x \geq 0 \tag{2.4}$$

and $I_0(x)$ is the first order Bessel function of the second kind. In (2.4), μ is a location parameter and represents the attenuation of the LOS path, while σ^2 is a scale parameter. The average channel attenuation is given by $2\sigma^2 + \mu^2$. The phase shift is once again uniformly distributed between $-\pi$ and π.

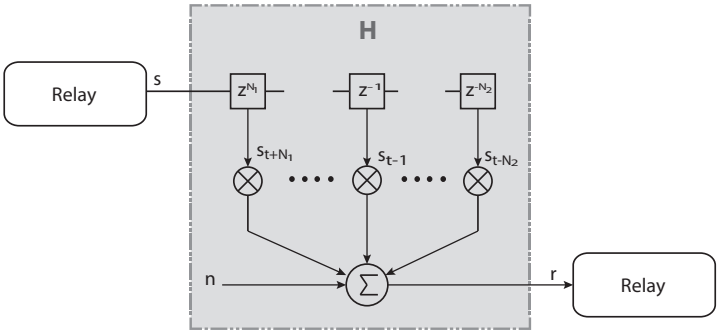

Figure 2.4: Multi-path channel model

The Rician/Rayleigh model accounts for local scattering of the signal at the receiver but, as the possible phase shift is limited to the range $[-\pi, \pi)$, it does not include the effects of ISI. More complex propagation models can account for received signals with varying amounts of delay by including additional paths with delayed versions of the transmitted signal. This model can now reproduce the effects of ISI where the received signal at a given time is dependent on multiple transmit

symbols. The properties of a variety of radio environments can be represented using combinations of path delays and expected attenuations. If the individual path gains are considered to be uncorrelated, the baseband signal can be described mathematically using a finite impulse response (FIR) structure

$$r_t = \sum_{n=-N_1}^{N_2} h_n \exp(\theta_n) s_{t-n},$$

where h_n and $\exp(\theta_n)$ make up the complex weights of the FIR filter. Details of how the weights are obtained are given in Sec. (4.2).

2.4.2 Radio Environments

The environment models used are taken from [23]. These specify power delay profiles based on measured data in a set of European locations designed to replicate the nature of propagation in general locations of a similar nature. The environments modeled are rural, urban, hilly rural and hilly urban scenarios. As a point of reference, a flat Rayleigh environment has also been simulated. The environment models are defined in Table 2.1. In the simulations the expected channel gains are normalized to unity. The models define a delay and a gain for each path with the shortest path assigned a delay of 0s and the strongest path a gain of 0dB. The sample period of the modulated signal is 21μs. The rural environment is the simplest radio environment with a small delay spread and half the signal power existing in a line of sight (LOS) path. This is representative of a high site situation where the relay nodes could be located on adjacent hilltops for example. The hilly rural environment has no LOS path and a much larger delay spread, 17μs at -12dB as opposed to 0.5μs at -20dB. This is representative of a situation such as a series of relays placed along the length of a valley. The urban environment includes a longest delay of 5μs at -10dB and the strongest path delayed by 0.2μs. The hilly urban environment has a sightly longer maximum delay of 6.6μs with the signal power more evenly distributed across the delay spread. It is important to consider a range of radio environments as different systems may be better suited to different environments.

Table 2.1: Delay spread parameters for radio models, delay in μs and power in dB

Tap	Rural		Urban		Hilly Urban		Hilly Rural	
	Delay	Power	Delay	Power	Delay	Power	Delay	Power
1	0	0	0	-3	0	-3	0	0
2	0.1	-4	0.2	0	0.4	0	0.2	-2
3	0.2	-8	0.6	-2	1.0	-3	0.4	-4
4	0.3	-12	1.6	-6	1.6	-5	0.6	-7
5	0.4	-16	2.4	-8	5.0	-2	15	-6
6	0.5	-20	5.0	-10	6.6	-4	17.2	-12

Considering the effect of multiple relay nodes on the end to end radio channel makes the propagation channel much more complex. To get a feel for the resulting channel, consider a SISO system with linear relays in the absence of noise. Starting with the flat Rayleigh case, when a set of these channels are combined in series the output becomes

$$r_t = \prod_n h_n s_t.$$

If we define the channel gain, h_n, in polar form, that is $h_n = A_n \exp(j\theta_n)$, the total phase change of the channel becomes $\sum_n \theta_n$. The combined amplitude is $\prod_n A_n$. Since $\sum_n \theta_n$ is the sum of N circularly symmetric, independent, uniformly distributed random variables it is also distributed uniformly in the interval $[-\pi, \pi)$. The combined amplitude is distributed as a product of Rayleigh variables.

Next we consider the multi-path channel model where

$$r_t = \sum_{n=-N_1}^{N_2} h_n \exp(\theta_n) s_{t-n}.$$

The combination of these channels becomes more cumbersome to describe mathematically. To circumvent this, first we define ϕ_d as a shift operator such that $\phi_d(s_t) = s_{t-d}$ and $\phi_{d_1}(s)\phi_{d_2}(s) = \phi_{d_1+d_2}(s)$. With this notation, the output can then be given as

$$r_t = \prod_{k=1}^{L} \left[\sum_{n=-N_1}^{N_2} h_n \exp(\theta_n) \phi_{d_{kn}}(s_t) \right].$$

The received signal is made up of the sum of all the possible products of L of

the original paths. Considering one of these path combinations, the amplitude is again distributed as a product of Rayleigh variables and the phase is uniform on the interval $[-\pi, \pi)$. Finally, the delay is the sum of the delays of the individual paths that make up the end to end paths. To assess the nature of the end to end channel it is useful to consider the power delay profile. That is the expected signal power at the receiver over time corresponding to an instance of a transmitted signal. For example, the power delay profile of the urban channel as defined in Table 2.1 is given in Fig. 2.5.

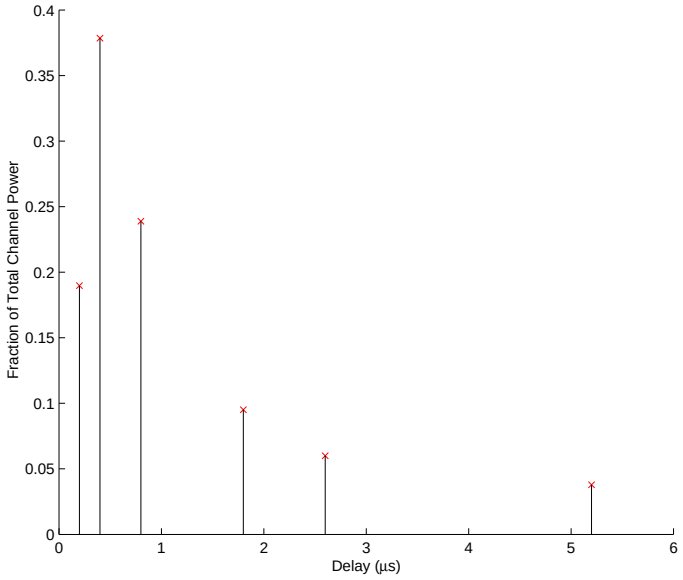

Figure 2.5: Power delay profile for urban environment

As these profiles define the transfer function of the channel the profile for multi-hop channels can be obtained by the convolution of the transfer functions. Figure 2.6 shows how the distribution of signal power in time is affected by multiple relay nodes.

As the number of hops increases, the dispersion of the signal in time increases. Without a receiver with the ability to equalize the channel, not only will the received power decrease as the transmitted power is spread outside the sample period, but this proportion of the transmitted power will also interfere with adjacent symbols. Furthermore issue can be exacerbated by non-coherent modulation schemes, as the

sample time at the receiver will not necessarily be aligned with the peak received power.

2.4.3 P25 Communications

We give special attention in this work to the P25 communication protocol. This uses a non-coherent frequency/differential phase modulation. The protocol maps 2 bits per symbol. While the P25 specification [24] allows some variation in the details of implementation, our system uses differential phase shift modulation. Here, the signal is represented by the change in phase between successive sample periods. The message bits are grey coded to symbols as given by the signal constellation in Table 2.2. The signal to be transmitted, s, is given by

Table 2.2: P25 signalling constellation

Bits	Phase Change
10	-135
00	-45
01	45
11	135

$$s_t = s_{t-1} \exp(i\theta_t),$$

where the subscript t gives the sample time and θ is the message symbol.

P25 communications have several advantages for wireless propagation. The constant envelope frequency/differential phase modulation is not susceptible to distortion due to a constant complex gain in the propagation path. Though the demodulated signal is affected by a time varying phase change in the propagation path, the extent of this effect is proportional to the rate of change of the channel phase and the symbol rate chosen for modulation. The protocol, being non-coherent and not taking advantage of any channel state information, will not provide a high bandwidth efficiency in challenging propagation environments. The payoff for this is low complexity radio hardware.

The symbol frequency is 4.8kHz, the modulation frequency 48kHz. The modulation frequency is higher than the symbol frequency as a higher modulation frequency

offers a higher level of robustness in fast fading channels. Conversely, the symbol frequency is lower than the modulation frequency, as this reduces susceptibility to ISI. The carrier frequency is 800MHz. To demodulate the received signal, the phase difference between successive samples is calculated and the result mapped back to the appropriate bits.

The receiver works as follows. The phase change between samples, $\hat{\theta}$, is obtained as,

$$\hat{\theta} = arg(r_t r_{t-1}^{\dagger}). \tag{2.5}$$

This phase change is then mapped to the closest valid symbol, that is the value of $m' \in \{-3, -1, 1, 3\}$ that minimizes

$$\left| arg\left(r_{it} r_{i(t-1)}^{*} \exp\left(\frac{-j\pi m'}{4} \right) \right) \right|.$$

The protocol also specifies a forward error correcting (FEC) scheme based on a convolution code. The code is based on a 96 symbol block and has a $\frac{1}{2}$ data rate. The symbols to be transmitted are interleaved before passing through the convolutional encoder and modulated as above. At the decoder, demodulation is performed as normal then a Viterbi decoder is used to estimate the interleaved symbols. These are then deinterleaved to recover the original symbol sequence.

2.4.4 Noise

The system is modeled using complex Gaussian noise. This is of the same form as used in the MIMO model. Hence the noise, n, is given by $\sqrt{\frac{N_0}{2}}(n_r + jn_i)$, where n_r and n_i are i.i.d real zero mean Gaussian variables and N_0 is the average noise power.

2.4.5 Relaying Protocol

The primary requirements of the relays are for them to be of low cost and power. This is the advantage it offers over a centrally routed (ie. base station) network. To achieve this goal the complexity of the relay nodes must remain low. Obviously,

maintaining a reasonable capacity over the link is also a requirement and this can become challenging as the number of relay nodes increase. To produce a practical communication system, the relay nodes must control the cumulative negative effects of the multi-hop propagation environment.

The simplest form of relay is a fixed gain amplifying relay in which $s_{l+1} = \alpha_l r_l$, where α_l is a constant scalar. In this type of system, the amplification factor, α_l, can be designed to control the expected transmit power, $E[|s_{l+1}|^2]$. To maintain a constant value for $E[|s_l|^2], l \in 1, 2, \ldots, L$, the amplification factor can be set as $\alpha_l = \sqrt{\frac{1}{E[|h_l|^2]+N_0}}$. This scheme will require expensive linear amplifiers. It also will prove unstable for channels with a large variance as there is no control over the instantaneous transmit powers, s_{l+1}^2. The scheme requires knowledge of the expected channel attenuations, $E[|h_l|^2]$, and expected noise power at the receiver, N_0.

If the relay is capable of tracking channel state information, a better system would use an adaptive gain, where $\alpha_l = \sqrt{\frac{1}{|h_l|^2+N_0}}$. A special case of this scheme can be applied to constant envelope modulation schemes. If no information is carried in the amplitude, the relay node can simply take the phase of the received signal and retransmit this at the desired power. Mathematically, this is equivalent to an amplification factor, $\alpha_l = \sqrt{\frac{1}{|r_l|^2}}$, and requires no knowledge of the channel state or received noise power. The fact the transmission power can be controlled precisely means the maximum power of information carrying signal can be transmitted at any given instance. Constant transmit power also allows the use of simple and cheap non-linear amplifiers.

Looking at decoding relays, the simplest relaying protocol detects message symbols then regenerates the estimated signal for transmission. This protocol requires a digital relay. In these relays the signal is shifted from pass band to base band and a differential detector is used to estimate the transmitted message symbols as per the P25 protocol. Differential modulation is then used to produce the signal imposed on the carrier signal for transmission. This also allows the transmit power to be precisely controlled. Hence this approach offers the same advantages of maximizing

the information carrying signal power and allowing the use of simple, non-linear amplifiers. There are other significant advantages to the decoding and regeneration of the message at each relay. It removes the effects of the multi-hop channel, only suffering from the results of channel distortion between each relay pair. The downside of this scheme is that any decoding errors at the relays will be propagated through to the final receiver.

The simulation work undertaken investigates four options for relaying protocols. These are referred to as Amplify and Forward (AF) [25], Phase Forwarding (PF), Detect and Regenerate (DetR) [26] and Decode and Regenerate (DecR). The AF protocol use the fixed amplification scheme giving a constant expected transmit power across all the relay nodes. PF relays use the phase only transmission scheme, providing constant power transmission. The DetR protocol is the basic digital relay, demodulating the input signal to perform symbol estimation before regenerating the signal for transmission. This protocol also allows constant power transmission. The DecR protocol is based on the trellis coded modulation (TCM) scheme of the P25 specification. In this case the relay nodes perform symbol detection in the same way as for DetR. Then, the most likely transmitted data sequence is estimated from the received symbols using a Viterbi algorithm. This estimate of the transmitted signal is then resent using the same convolutional code.

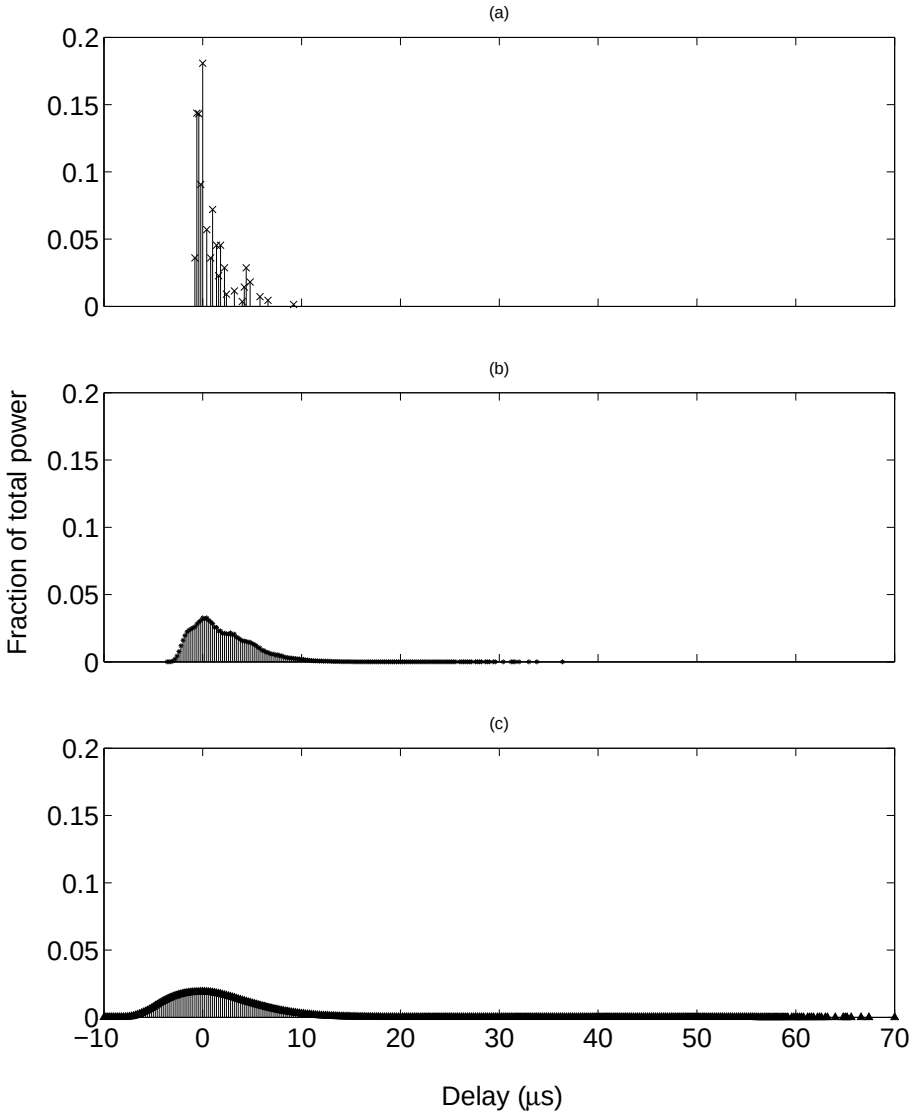

Figure 2.6: Power delay profile for urban multi-hop channels, the two hop profile is given in (a), 8 hop in (b), 16 hop in (c).

Chapter 3

Statistical Properties of Multi-hop Relay Chains

This analysis of relay chains focuses on the use of linear relays in flat Rayleigh radio environments. The flat Rayleigh model is used as this is the most important baseline case and leads to a multiplicative channel model, as opposed to requiring a convolution operation which results from the use of a multi-path model. As the statistics of the flat Rayleigh case are already highly complex, the multi-path case has been left to be considered in future work. Detect and regenerate relays are also not considered in this section. The reason for this is that in decoding relays the message is regenerated at each relay and so the problem becomes one of error propagation and the propagation channel between each relay pair can be handled independently. To recap the system model presented in Sec. 2.3, the communication system is represented at the l^{th} relay by

$$\begin{aligned} \mathbf{s}_{l+1} &= \alpha_l \mathbf{r}_l \\ &= \alpha_l(\mathbf{H}_l \mathbf{s}_l + \mathbf{n}_l). \end{aligned}$$

In Secs. 3.3-3.5 the linear amplification term, α, is left arbitrary. To give explicit results in these sections we assume that it is a constant.

The focus of this section is the development of an end to end system model, of the form $\mathbf{r}_L = \mathbf{H}_{eq}\mathbf{s}_1 + \mathbf{n}_{eq}$. Ideally this will prove useful in analysis of properties such as end to end capacity and BER. An end to end model is found for a multiple input

single output (MISO) system. We use this to characterise end to end properties including noise to signal ratios and the moments of elements of the channel matrix and noise vector. Additionally, the dependence structure in the end to end model is established for MIMO systems. Finally, a characterisation of the eigenvalues of a MIMO system is presented.

3.1 Equivalent Channel Matrices

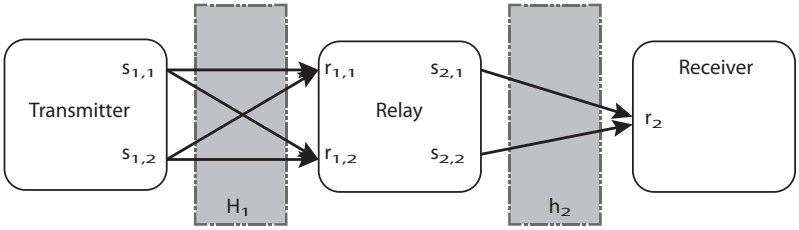

Figure 3.1: Example of a simple MISO system

Here we construct an end to end model for a MISO system. This can also be applied to a MIMO system to give properties relating to a single receive antenna. Consider a MISO system in the context of a relay chain. Here, arrays of antennas at the source and relays transmit to arrays of receive antennas, with the constraint that the final receiver has only one antenna. This reduces the channel matrix between the final relay and receiver to a vector. We will look at a specific case of this type of system to illustrate the method of obtaining the equivalent model. Consider a system using a 2×2 MIMO link followed by a single antenna receiver, as in Fig. 3.1, with a flat Rayleigh channel and linear relaying. For this example we have the channel model,

$$r_2 = \begin{bmatrix} h_{2,1} & h_{2,2} \end{bmatrix} \alpha_1 \left(\begin{bmatrix} (H_1)_{1,1} & (H_1)_{1,2} \\ (H_1)_{2,1} & (H_1)_{2,2} \end{bmatrix} \begin{bmatrix} s_{1,1} \\ s_{1,2} \end{bmatrix} + \begin{bmatrix} n_{1,1} \\ n_{1,2} \end{bmatrix} \right) + n_2. \tag{3.1}$$

This can be written as

$$\begin{aligned} r_2 \;&= \alpha_1 \begin{bmatrix} h_{2,1}(H_1)_{1,1} + h_{2,2}(H_1)_{2,1} & h_{2,1}(H_1)_{1,2} + h_{2,2}(H_1)_{2,2} \end{bmatrix} \begin{bmatrix} s_{1,1} \\ s_{1,2} \end{bmatrix} \\ &\quad + \alpha_1 \begin{bmatrix} h_{2,1} n_{1,1} + h_{2,2} n_{1,2} \end{bmatrix} + n_2 \end{aligned} \tag{3.2}$$

It is well known [21, Chap. 13, Sec. 3] that a linear combination of ZMCSCG variables is equivalent to a single ZMCSCG variable. In particular, for a linear combination of two ZMCSCG variables we have

$$az_1 + bz_2 = \left(\sqrt{|a|^2 + |b|^2}\right) z_3,$$

where z_1, z_2, z_3 are i.i.d $\mathbb{C}N(0,1)$. Hence, conditioning on $h_{2,1}$ and $h_{2,2}$, r_2 can be rewritten as

$$r_2 = \alpha_1 \begin{bmatrix} \sqrt{|h_{2,1}|^2 + |h_{2,2}|^2} z_1 & \sqrt{|h_{2,1}|^2 + |h_{2,2}|^2} z_2 \end{bmatrix} \begin{bmatrix} s_{1,1} \\ s_{1,2} \end{bmatrix} + \alpha_1 \sqrt{|h_{2,1}|^2 + |h_{2,2}|^2} z_3 + n_2. \tag{3.3}$$

Equation (3.3) can be simplified by using the result that a sum of squares of real Gaussian variables is distributed as a chi square random variable with the degrees of freedom given by the number of Gaussian variables in the sum [21, Chap. 18]. Hence, the term $|h_{2,1}|^2 + |h_{2,2}|^2$ in (3.3) is distributed as a chi square random variable. Both $|h_{2,1}|^2$ and $|h_{2,1}|^2$ are distributed as the sum of two real Gaussian variables, with variance of a half, squared. This means that $|h_{2,1}|^2 + |h_{2,2}|^2$ is distributed as half of a chi square variable, X_1, with four degrees of freedom. Therefore, r_2 has the representation,

$$\begin{aligned} r_2 \;&= \alpha_1 \begin{bmatrix} \sqrt{\frac{X_1}{2}} z_1 & \sqrt{\frac{X_1}{2}} z_2 \end{bmatrix} \begin{bmatrix} s_{1,1} \\ s_{1,2} \end{bmatrix} + \alpha_1 \sqrt{\frac{X_1}{2}} z_3 + n_2, \\ &= \alpha_1 \sqrt{\frac{X_1}{2}} \left(\begin{bmatrix} z_1 & z_2 \end{bmatrix} \begin{bmatrix} s_{1,1} \\ s_{1,2} \end{bmatrix} + z_3 \right) + n_2. \end{aligned} \tag{3.4}$$

This approach can be extended to three hops. The full channel model for this system is,

$$\begin{aligned} r_2 &= \begin{bmatrix} h_{3,1} & h_{3,2} \end{bmatrix} \alpha_2 \\ &\times \left(\begin{bmatrix} (H_2)_{1,1} & (H_2)_{1,2} \\ (H_2)_{2,1} & (H_2)_{2,2} \end{bmatrix} \alpha_1 \left(\begin{bmatrix} (H_1)_{1,1} & (H_1)_{1,2} \\ (H_1)_{2,1} & (H_1)_{2,2} \end{bmatrix} \begin{bmatrix} s_{1,1} \\ s_{1,2} \end{bmatrix} + \begin{bmatrix} n_{1,1} \\ n_{1,2} \end{bmatrix} \right) + \begin{bmatrix} n_{2,1} \\ n_{2,2} \end{bmatrix} \right) \\ &+ n_3 \end{aligned} \tag{3.5}$$

Let,

$$\begin{bmatrix} v_1 \\ v_2 \end{bmatrix} = \alpha_1 \left(\begin{bmatrix} (H_1)_{1,1} & (H_1)_{1,2} \\ (H_1)_{2,1} & (H_1)_{2,2} \end{bmatrix} \begin{bmatrix} s_{1,1} \\ s_{1,2} \end{bmatrix} + \begin{bmatrix} n_{1,1} \\ n_{1,2} \end{bmatrix} \right),$$

then substituting this into (3.5) gives

$$r_2 = \begin{bmatrix} h_{3,1} & h_{3,2} \end{bmatrix} \alpha_2 \left(\begin{bmatrix} (H_2)_{1,1} & (H_2)_{1,2} \\ (H_2)_{2,1} & (H_2)_{2,2} \end{bmatrix} \begin{bmatrix} v_1 \\ v_2 \end{bmatrix} + \begin{bmatrix} n_{2,1} \\ n_{2,2} \end{bmatrix} \right) + n_3. \tag{3.6}$$

Equation (3.6) is of the same form as (3.1). Hence, using the same argument as above, this can be reduced to,

$$r_2 = \alpha_2 \sqrt{\frac{X_2}{2}} \left(\begin{bmatrix} z_1 & z_2 \end{bmatrix} \begin{bmatrix} v_1 \\ v_2 \end{bmatrix} + z_3 \right) + n_3, \tag{3.7}$$

where $X_2 = 2(|h_{3,1}|^2 + |h_{3,2}|^2)$. Substituting,

$$\begin{bmatrix} v_1 \\ v_2 \end{bmatrix} = \alpha_1 \left(\begin{bmatrix} (H_1)_{1,1} & (H_1)_{1,2} \\ (H_1)_{2,1} & (H_1)_{2,2} \end{bmatrix} \begin{bmatrix} s_{1,1} \\ s_{1,2} \end{bmatrix} + \begin{bmatrix} n_{1,1} \\ n_{1,2} \end{bmatrix} \right),$$

back into (3.7), gives

$$r_2 = \alpha_2 \sqrt{\frac{X_2}{2}} \left(\begin{bmatrix} z_1 & z_2 \end{bmatrix} \alpha_1 \left(\begin{bmatrix} (H_1)_{1,1} & (H_1)_{1,2} \\ (H_1)_{2,1} & (H_1)_{2,2} \end{bmatrix} \begin{bmatrix} s_{1,1} \\ s_{1,2} \end{bmatrix} + \begin{bmatrix} n_{1,1} \\ n_{1,2} \end{bmatrix} \right) + z_3 \right) + n_3.$$

Now the term given by

$$\left(\begin{bmatrix} z_1 & z_2 \end{bmatrix} \alpha_1 \left(\begin{bmatrix} (H_1)_{1,1} & (H_1)_{1,2} \\ (H_1)_{2,1} & (H_1)_{2,2} \end{bmatrix} \begin{bmatrix} s_{1,1} \\ s_{1,2} \end{bmatrix} + \begin{bmatrix} n_{1,1} \\ n_{1,2} \end{bmatrix} \right) + z_3 \right),$$

is of the same form as (3.1). Therefore, this can again be reduced to

$$r_2 = \alpha_2\sqrt{\frac{X_2}{2}}\left(\alpha_1\sqrt{\frac{X_1}{2}}\left(\begin{bmatrix} z_4 & z_5 \end{bmatrix}\begin{bmatrix} s_{1,1} \\ s_{1,2} \end{bmatrix} + z_6\right) + z_3\right) + n_3, \tag{3.8}$$

where $X_1 = 2(|z_1|^2 + |z_2|^2)$.

To extend this argument to an arbitrary number of hops we first express the channel model in a form more conducive to arbitrary hop lengths. To do this, the signal and noise components of the channel are separated as follows. For the two hop case,

$$\begin{aligned} r_2 &= \mathbf{h}_2\alpha_1(\mathbf{H}_1\mathbf{s}_1 + \mathbf{n}_1) + n_2 \\ &= \alpha_1\mathbf{h}_2\mathbf{H}_1\mathbf{s}_1 + \alpha_1\mathbf{h}_2\mathbf{n}_1 + n_2 \\ &= \textstyle\prod_{l=1}^{1}\alpha_l\prod_{l=1}^{2}\mathbf{H}_l\mathbf{s}_1 + \sum_{l=1}^{2}\prod_{k=l}^{1}\alpha_k\prod_{k=l+1}^{2}\mathbf{H}_k\mathbf{n}_l, \end{aligned}$$

where it is understood that $\mathbf{H}_2 = \mathbf{h}_2$ and $\prod_{l=1}^{2}\mathbf{H}_l = \mathbf{H}_2\mathbf{H}_1 = \mathbf{h}_2\mathbf{H}_1$. With similar notation for three hops we have,

$$\begin{aligned} r_3 &= \mathbf{h}_3\alpha_2(\mathbf{H}_2\alpha_1(\mathbf{H}_1\mathbf{s}_1 + \mathbf{n}_1) + \mathbf{n}_2) + n_3 \\ &= \alpha_2\alpha_1\mathbf{h}_3\mathbf{H}_2\mathbf{H}_1\mathbf{s}_1 + \alpha_2\alpha_1\mathbf{h}_3\mathbf{H}_2\mathbf{n}_1 + \alpha_2\mathbf{h}_3\mathbf{n}_2 + n_3 \\ &= \textstyle\prod_{l=1}^{2}\alpha_l\prod_{l=1}^{3}\mathbf{H}_l\mathbf{s}_1 + \sum_{l=1}^{3}\prod_{k=l}^{2}\alpha_k\prod_{k=l+1}^{3}\mathbf{H}_k\mathbf{n}_l. \end{aligned}$$

Finally with L hops,

$$r_L = \prod_{l=1}^{L-1}\alpha_l\prod_{l=1}^{L}\mathbf{H}_l\mathbf{s}_1 + \sum_{l=1}^{L}\prod_{k=l}^{L-1}\alpha_k\prod_{k=l+1}^{L}\mathbf{H}_k\mathbf{n}_l. \tag{3.9}$$

To reduce this to the simplified model, as in (3.4) and (3.8), we expand this expression as follows,

$$\begin{aligned} r_L = \;& \mathbf{h}_L\alpha_{L-1} \\ & \times(\mathbf{H}_{L-1}\alpha_{L-2}(\textstyle\prod_{l=1}^{L-3}\alpha_l\prod_{l=1}^{L-2}\mathbf{H}_l\mathbf{s}_1 + \sum_{l=1}^{L-2}\prod_{k=l}^{L-3}\alpha_k\prod_{k=l+1}^{L-2}\mathbf{H}_k\mathbf{n}_l) + \mathbf{n}_{L-1}) \\ & + n_L \end{aligned} \tag{3.10}$$

Let $\prod_{l=1}^{L-3}\alpha_l\prod_{l=1}^{L-2}\mathbf{H}_l\mathbf{s}_1 + \sum_{l=1}^{L-2}\prod_{k=l}^{L-3}\alpha_k\prod_{k=l+1}^{L-2}\mathbf{H}_k\mathbf{n}_l = \mathbf{v}_{L-2}$, then

$$r_L = \mathbf{h}_L \alpha_{L-1}(\mathbf{H}_{L-1}\alpha_{L-2}\mathbf{v}_{L-2} + \mathbf{n}_{L-1}) + n_L.$$

This is of the same form as (3.1) and following the same argument as above can be expressed as

$$r_L = \alpha_{L-1}\sqrt{\frac{X_L}{2}}(\mathbf{z}_{L-1}\alpha_{L-2}\mathbf{v}_{L-2} + n_{L-1}) + n_L.$$

Repeating this process we can write,

$$\begin{aligned} r_L &= \alpha_{L-1}\sqrt{\tfrac{X_L}{2}}(\mathbf{z}_{L-1}\alpha_{L-2}(\mathbf{H}_{L-2}\alpha_{L-3}\mathbf{v}_{L-3} + \mathbf{n}_{L-2}) + n_{L-1}) + n_L \\ &= \alpha_{L-1}\sqrt{\tfrac{X_L}{2}}(\alpha_{L-2}\sqrt{\tfrac{X_{L-1}}{2}}(\mathbf{z}_{L-2}\alpha_{L-3}\mathbf{v}_{L-3} + n_{L-2}) + n_{L-1}) + n_L \\ &= \textstyle\prod_{l=2}^{L}\alpha_{l-1}\sqrt{\frac{X_l}{2}}\mathbf{z_1}\mathbf{s}_1 + \sum_{l=1}^{L}\prod_{k=l+1}^{L}\alpha_{k-1}\sqrt{\frac{X_k}{2}}n_l. \end{aligned} \tag{3.11}$$

From (3.11) we can now define expressions for the equivalent channel matrix and noise terms. These are given by,

$$\mathbf{h}_{eq} = \prod_{l=2}^{L}\alpha_{l-1}\sqrt{\frac{X_l}{2}}\mathbf{z_1},$$

$$n_{eq} = \sum_{l=1}^{L}\prod_{k=l+1}^{L}\alpha_{k-1}\sqrt{\frac{X_k}{2}}n_l.$$

The expression for n_{eq} can be further simplified by combining the N i.i.d ZMCSCG noise variables, $n_l, l \in \{1, 2, \ldots, N\}$, into a single ZMCSCG variable with an equivalent distribution. Its variance, given by the sum of the variances of $n_l, l \in \{1, 2, \ldots, N\}$, is $\sum_{l=1}^{L}\prod_{k=l+1}^{L}\alpha_{k-1}^2\frac{X_k}{2}$. Hence,

$$n_{eq} = \left(\sqrt{\sum_{l=1}^{L}\prod_{k=l+1}^{L}\alpha_{k-1}^2\frac{X_k}{2}}\right)z,$$

where z is an independent ZMCSCG variable.

Unfortunately, this approach can not be applied quite so effectively to a MIMO or SIMO system. With multiple outputs the channel matrix develops a complex dependence structure that cannot be reproduced using the chi square model. In a SIMO system we can look at the information carrying component of the received signal in isolation. The equivalent channel can be expressed in a similar way as

$$\mathbf{h}_{eq} = \prod_{l=2}^{L} \alpha_{l-1}\mathbf{H}_l\mathbf{h}_1.$$

Using a similar approach to the MISO case we let $\|\mathbf{h}_1\|^2 = \frac{X_1}{2}$ and substitute $\mathbf{H}_2\mathbf{h}_1$ with the equivalent distribution $\mathbf{z}_2\sqrt{\frac{X_1}{2}}$ giving,

$$\mathbf{h}_{eq} = \prod_{l=3}^{L} \alpha_{l-1}\mathbf{H}_l\mathbf{z}_2\alpha_1\sqrt{\frac{X_1}{2}}.$$

Repeating this procedure gives the general expression

$$\mathbf{h}_{eq} = \mathbf{z}_L \prod_{l=1}^{L-1} \alpha_l\sqrt{\frac{X_l}{2}}.$$

Hence, $\mathbf{h}_{eq}$ has a simple form but the problem arises with the noise component of the equivalent channel model. For the equivalent noise, we can write

$$\mathbf{n}_{eq} = \sum_{l=1}^{L} \prod_{k=l}^{L-1} \prod_{k=l+1}^{L} \mathbf{H}_k\mathbf{n}_l, \tag{3.12}$$

From (3.12) we observe that the noise terms do not involve the vector channel $\mathbf{h}_1$, which is essential in simplifying the structure of the equivalent channel vector.

The same problem arises in a full MIMO system. In this case, some properties of the channel can be obtained by considering a single receiver in isolation. The model is then equivalent to the single output case. In an $M \times N$ MIMO system with L hops, the received signal is given by,

$$\mathbf{r}_L = \prod_{l=1}^{L-1} \alpha_l \prod_{l=1}^{L} \mathbf{H}_l\mathbf{s}_1 + \sum_{l=1}^{L} \prod_{k=l}^{L-1} \alpha_k \prod_{k=l+1}^{L} \mathbf{H}_k\mathbf{n}_l.$$

Hence the signal at the m^{th} receive antenna is given by,

$$\begin{aligned}(\mathbf{r}_L)_m &= (\mathbf{H}_L)_m\alpha_{L-1}\left(\textstyle\prod_{l=1}^{L-2}\alpha_l\prod_{l=1}^{L-1}\mathbf{H}_l\mathbf{s}_1 + \sum_{l=1}^{L-1}\prod_{k=1}^{L-2}\alpha_k\prod_{k=l+1}^{L-1}\mathbf{H}_k\mathbf{n}_l\right) + n_L \\ &= (\mathbf{H}_L)_m\alpha_{L-1}\times \\ &\left(\mathbf{H}_{L-1}\alpha_{L-2}\left(\textstyle\prod_{l=1}^{L-3}\alpha_l\prod_{l=1}^{L-2}\mathbf{H}_l\mathbf{s}_1 + \sum_{l=1}^{L-w}\prod_{k=l}^{L-3}\alpha_k\prod_{k=l+1}^{L-2}\mathbf{H}_k\mathbf{n}_l\right) + \mathbf{n}_{L-1}\right) \\ &+n_L.\end{aligned} \tag{3.13}$$

Equation (3.13) is of the same structure as (3.10) so can be written as

$$(r_L)_m = \prod_{l=2}^{L} \alpha_{l-1} \sqrt{\frac{X_l}{2}} \mathbf{z_1 s_1} + \left(\sqrt{\sum_{l=1}^{L} \prod_{k=l+1}^{L} \alpha_{k-1}^2 \frac{X_k}{2}} \right) n. \tag{3.14}$$

This expression will allow the statistics of a single row of the equivalent channel and noise component to be calculated.

In summary, (3.11) gives an end to end system model for a MISO system. The same system model can also be applied when considering a single receive antenna in a MIMO system. For this case the end to end model is given by (3.14).

3.2 Dependence Structure of the End to End System

In this section we establish the dependence between components of the system model for a MIMO relay chain. First we will look at the correlation of elements of $\mathbf{H}_{eq}$. For this analysis we will limit ourselves to linear relays that only posses knowledge of the channel properties before them in the relay chain. That is, α_l is only dependent on $\mathbf{H}_k, k < l$. Consider the element $(H_{eq})_{mn}$ given by

$$\begin{aligned} (H_{eq})_{mn} &= (\mathbf{H}_L)_m (\textstyle\prod_{l=1}^{L-1} \alpha_l \mathbf{H}_l)_n \\ &= \textstyle\sum_{u=1}^{M} (H_L)_{mu} (\prod_{l+1}^{L-1} \alpha_l \mathbf{H}_l)_{un}. \end{aligned}$$

With this representation, consider the correlation

$$\begin{aligned} E[(H_{eq})_{mn}(H_{eq})^\dagger_{uv}] &= E[\left(\textstyle\sum_{a=1}^{M} (H_L)_{ma} (\prod_{l+1}^{L-1} \alpha_l \mathbf{H}_l)_{an}\right) \left(\sum_{b=1}^{M} (H_L)_{ub} (\prod_{l+1}^{L-1} \alpha_l \mathbf{H}_l)_{bv}\right)^\dagger] \\ &= E[\textstyle\sum_{a,b=1}^{M} (H_L)_{ma} (H_L)^\dagger_{ub} (\prod_{l+1}^{L-1} \alpha_l \mathbf{H}_l)_{an} (\prod_{l+1}^{L-1} \alpha_l \mathbf{H}_l)^\dagger_{bv}] \\ &= \textstyle\sum_{a,b=1}^{M} E[(H_L)_{ma}] E[(H_L)^\dagger_{ub}] E[(\prod_{l+1}^{L-1} \alpha_l \mathbf{H}_l)_{an} (\prod_{l+1}^{L-1} \alpha_l \mathbf{H}_l)^\dagger_{bv}]. \end{aligned}$$

Since $(H_L)_{ma}$ is a ZMCSCG variable with $E[(H_L)_{ma}] = 0$, we have

$$E[(H_{eq})_{mn}(H_{eq})^\dagger_{uv}] = 0.$$

While the components of the channel matrix are uncorrelated they are not necessarily independent. For the two hop case, where $(H_{eq})_{ij} = (\mathbf{H}_2)_i (\mathbf{H}_1)_j$, components

from the same column of $\mathbf{H}_{eq}$ will depend on the same column of $\mathbf{H}_1$. Components from the same row of $\mathbf{H}_{eq}$ will depend on the same row of $\mathbf{H}_2$. In a system with L hops, $(H_{eq})_{ij} = (\mathbf{H}_L)_i \prod_{l=2}^{L-1} \mathbf{H}_l (\mathbf{H}_1)_j$. Hence all components of $\mathbf{H}_{eq}$ will be dependent on $\prod_{l=2}^{L-1} \mathbf{H}_l$. This complex dependence structure, without correlation, makes it difficult to develop a direct representation for $\mathbf{H}_{eq}$ in the multiple output case. In the single output case, the dependence is represented by the product of chi square variables.

In the multiple output case the equivalent noise term is a vector, as opposed to the scalar term in the single output system. The same questions about correlation and dependence within the noise vector can also be asked. To investigate this issue we consider

$$
\begin{aligned}
&E[\mathbf{n}_{eq,u}\mathbf{n}_{eq,v}^{\dagger}] \\
&= E[\Big(n_{L,u} + \textstyle\sum_{k=1}^{L-1}(\mathbf{H}_L)_u(\prod_{l=k+1}^{L-1}\alpha_l\mathbf{H}_l n_k)\Big)\Big(n_{L,v} + \sum_{k=1}^{L-1}(\mathbf{H}_L)_v(\prod_{l=k+1}^{L-1}\alpha_l\mathbf{H}_l n_k)^{\dagger}\Big)] \\
&= E[\textstyle\sum_{a,b=1}^{L-1}(\mathbf{H}_L)_u(\prod_{l=a+1}^{L-1}\alpha_l\mathbf{H}_l n_a)(\prod_{l=b+1}^{L-1}\alpha_l\mathbf{H}_l n_b)^{\dagger}(\mathbf{H}_L)_v^{\dagger} \\
&+ \textstyle\sum_{b=1}^{L-1} n_{L,u}(\prod_{l=b+1}^{L-1}\alpha_l\mathbf{H}_l n_b)^{\dagger}(\mathbf{H}_L)_v^{\dagger} \\
&+ \textstyle\sum_{a=1}^{L-1} n_{L,v}^{\dagger}(H_L)_u(\prod_{l=a+1}^{L-1}\alpha_l\mathbf{H}_l n_a) + n_{L,u}n_{L,v}^{\dagger}] \\
&= \textstyle\sum_{a,b=1}^{L-1} E[(\mathbf{H}_L)_u(\prod_{l=a+1}^{L-1}\alpha_l\mathbf{H}_l n_a)(\prod_{l=b+1}^{L-1}\alpha_l\mathbf{H}_l n_b)^{\dagger}(\mathbf{H}_L)_v^{\dagger}] \\
&+ \textstyle\sum_{b=1}^{L-1} E[n_{L,u}(\prod_{l=b+1}^{L-1}\alpha_l\mathbf{H}_l n_b)^{\dagger}(\mathbf{H}_L)_v^{\dagger}] \\
&+ \textstyle\sum_{a=1}^{L-1} E[n_{L,v}^{\dagger}(H_L)_u(\prod_{l=a+1}^{L-1}\alpha_l\mathbf{H}_l n_a)] + E[n_{L,u}n_{L,v}^{\dagger}].
\end{aligned}
\tag{3.15}
$$

Separating each of the three expectations in (3.15) we have

$$
\begin{aligned}
&E[(\mathbf{H}_L)_u(\textstyle\prod_{l=a+1}^{L-1}\alpha_l\mathbf{H}_l n_a)(\prod_{l=b+1}^{L-1}\alpha_l\mathbf{H}_l n_b)^{\dagger}(\mathbf{H}_L)_v^{\dagger}] \\
&= E[\textstyle\sum_{k=1}^{M}(H_L)_{uk}(\prod_{l=a+1}^{L-1}\alpha_l\mathbf{H}_l n_a)_k(\prod_{l=b+1}^{L-1}\alpha_l\mathbf{H}_l n_b)_k^{\dagger}(H_L)_{vk}^{\dagger}] \\
&= \textstyle\sum_{k=1}^{M} E[(H_L)_{uk}(H_L)_{vk}^{\dagger}(\prod_{l=a+1}^{L-1}\alpha_l\mathbf{H}_l n_a)_k(\prod_{l=b+1}^{L-1}\alpha_l\mathbf{H}_l n_b)_k^{\dagger}] \\
&= \textstyle\sum_{k=1}^{M} E[(H_L)_{uk}]E[(H_L)_{vk}^{\dagger}]E[(\prod_{l=a+1}^{L-1}\alpha_l\mathbf{H}_l n_a)_k(\prod_{l=b+1}^{L-1}\alpha_l\mathbf{H}_l n_b)_k^{\dagger}]
\end{aligned}
$$

when $u \neq v$. As $(H_L)_{uk}$ is a ZMCSCG variable $E[(H_L)_{uk}] = 0$ and

$$
E[(\mathbf{H}_L)_u(\prod_{l=a+1}^{L-1}\alpha_l\mathbf{H}_l n_a)(\prod_{l=b+1}^{L-1}\alpha_l\mathbf{H}_l n_b)^{\dagger}(\mathbf{H}_L)_v^{\dagger}] = 0, u \neq v.
$$

Next

$$E[n_{L,u}(\prod_{l=b+1}^{L-1}\alpha_l\mathbf{H}_l n_b)^\dagger(\mathbf{H}_L)_v^\dagger] = 0$$

as $n_{L,u}$ is an independent ZMCSCG variable.

Finally,

$$E[n_{L,u}n_{L,v}^\dagger] = 0, u \neq v,$$

as $n_{L,u}$ and $n_{L,v}$ are independent ZMCSCG variables, when $u \neq v$. Hence $E[\mathbf{n}_{eq,u}\mathbf{n}_{eq,v}^\dagger] = 0$, $u \neq v$.

As for dependence, from the above equations we can see that all components of the noise vector contain the terms $\mathbf{H}_l, l \in \{2, 3, \ldots, L-1\}$. Hence they will exhibit some degree of dependence. More importantly, this also demonstrates a dependence between $\mathbf{H}_{eq}$ and $\mathbf{n}_{eq}$.

In summary, while the elements of $\mathbf{H}_{eq}$ are uncorrelated they are dependent on one another. Similarly $\mathbf{n}_{eq}$ also contains uncorrelated yet dependent elements. In addition, the channel matrix, $\mathbf{H}_{eq}$, and noise vector, $\mathbf{n}_{eq}$, are also dependent.

3.3 Moments of equivalent noise and channel matrices

Here we develop an expression for the moments of elements of the equivalent channel matrix and noise vector. First, we will look at $E[|(H_{eq})_{mn}|^r]$, for a system with L relay hops, M receive antennas and N transmit antennas, with $r \in \mathbb{Z}^+$. Using (3.14) we can write

$$(H_{eq})_{mn} = \prod_{l=2}^{L}\alpha_l\sqrt{\frac{X_l}{2}}z_n,$$

where $X_l, l \in \{2, 3, \ldots, L\}$ are i.i.d chi square random variables with $2N$ degrees of freedom and z_n is a ZMCSCG variable. With these properties

$$E[|(H_{eq})_{mn}|^r] = \prod_{l=2}^{L} \alpha_l^r E\left[\left(\frac{X_l}{2}\right)^{\frac{r}{2}}\right] E[|z_n|^r].$$

The problem is now one of establishing the value of $E[\left(\frac{X_l}{2}\right)^{\frac{r}{2}}]$ and $E[|z_n|^r]$. The result for $E[|z_n|^r]$ is readily available in standard statistics references [21, Chap. 13, Sec. 3] as below

$$\begin{aligned} E[|z_n|^r] &= 0, \text{ for odd } r \\ &= r!, \text{ for even } r. \end{aligned}$$

Given this result,

$$E[|(H_{eq})_{mn}|^r] = 0, \text{ for odd } r,$$

and we need only consider $E[\left(\frac{X_l}{2}\right)^r]$. The moments for a standard chi square variable are given in [21, Chap. 18, Sec. 3] as

$$E[X_l^r] = 2^r \frac{(N+r-1)!}{(N-1)!}.$$

Since

$$E\left[\left(\frac{X_l}{2}\right)^r\right] = \left(\frac{1}{2}\right)^r E[X_l^r],$$

it follows that

$$E\left[\left(\frac{X_l}{2}\right)^r\right] = \frac{(N+r-1)!}{(N-1)!}.$$

Using these results we can now write

$$\begin{aligned} E[|(H_{eq})_{mn}|^{2r}] &= \left[\prod_{l=2}^{L} \alpha_l^{2r} \left(\tfrac{(N+r-1)!}{(N-1)!}\right)\right] r! \\ &= \left[\prod_{l=2}^{L} \alpha_l^{2r}\right] r! \left(\tfrac{(N+r-1)!}{(N-1)!}\right)^{L-1}. \end{aligned} \tag{3.16}$$

The moments of the equivalent noise term are more complicated due to the sums of products involved. Taking the representation for $n_{eq,m}$ in (3.14), two simpler results can be obtained first:

$$E[|n_{eq,m}|^r] = E\left[\left(\sqrt{\sum_{l=1}^{L} \prod_{k=l+1}^{L} \alpha_{k-1}^2 \frac{X_k}{2}}\right)^r\right] E[N_0|z_u|^r],$$

which is zero for odd r, as $E[|z_u|^r] = 0$ for odd r. The second of these results is the second moment which can be found as follows.

$$\begin{aligned} E[|n_{eq,m}|^2] &= E\left[\sum_{l=1}^{L}\prod_{k=l+1}^{L}\alpha_{k-1}^2\frac{X_k}{2}\right]E[N_0|z_u|^2] \\ &= \left[\sum_{l=1}^{L}E\left[\prod_{k=l+1}^{L}\alpha_{k-1}^2\frac{X_k}{2}\right]\right]E[N_0|z_u|^2] \\ &= N_0\sum_{l=1}^{L}\left(\prod_{k=l+1}^{L}\alpha_{k-1}^2 E\left[\frac{X_k}{2}\right]\right) \\ &= N_0\sum_{l=1}^{L}\left(\prod_{k=l+1}^{L}\alpha_{k-1}^2\right)\left(\frac{(N+r-1)!}{(N-1)!}\right)^{L-l}. \end{aligned}$$

To find moments greater then the second, we need to evaluate $E\left[\left(\sum_{l=1}^{L}\prod_{k=l+1}^{L}\alpha_{k-1}^2\frac{X_k}{2}\right)^r\right]$. To simplify notation, the multinomial conventions will be used to expand this expression.

The multinomial notation is an extension of the binomial convention to systems of multiple variables. An example of its use would be the expansion of a power of a sum, such as $\left(\sum_i v_i\right)^R$, to

$$\left(\sum_i v_i\right)^R = \sum_{|\mathbf{r}|=R}\binom{R}{\mathbf{r}}\prod_{i=1}^{L}v_i^{r_i},$$

where L is the dimension of $\mathbf{v} = \begin{pmatrix} v_1 & v_2 & \dots & v_L \end{pmatrix}$ and $\mathbf{r} = \begin{pmatrix} r_1 & r_2 & \dots & r_L \end{pmatrix}$. The multinomial coefficient $\binom{R}{\mathbf{r}}$ is defined as $\frac{R!}{\prod_{i=1}^{L} r_i!}$. The sum is taken over all permutations of the vector $\mathbf{r}$ such that $|\mathbf{r}| = R$.

Using the notation $Xp_k = \prod_{l=k}^{L}\alpha_{l-1}^2\frac{X_l}{2}$, combined with the multinomial notation we can write

$$\left(\sum_{l=1}^{L}\prod_{k=l+1}^{L}\alpha_{k-1}^2 X_k^2\right)^r = \sum_{|\mathbf{k}|=r}\binom{r}{\mathbf{k}}\prod_{i=1}^{L}Xp_{i+1}^{k_i}.$$

The need now is to establish the value of $E[\prod_{i=1}^{L}Xp_{i+1}^{k_i}]$. From the definition of Xp_i it follows that $\prod_{i=1}^{L}(Xp_{i+1})^{k_i} = \prod_{i=2}^{L+1}\left(\alpha_{i-1}^2\frac{X_i}{2}\right)^{\sum_{j=L+1-i}^{L-1}k_j}$. Hence,

$$\begin{aligned} E[\textstyle\prod_{i=1}^{L}Xp_{i+1}^{k_i}] &= \textstyle\prod_{i=2}^{L+1}\alpha_{i-1}^{2\sum_{j=L+1-i}^{L-1}k_j}E[\left(\frac{X_i}{2}\right)^{\sum_{j=L+1-i}^{L-1}k_j}] \\ &= \left[\textstyle\prod_{i=2}^{L+1}\alpha_{i-1}^{2\sum_{j=L+1-i}^{L-1}k_j}\right]\frac{(N+\sum_{j=L+1-i}^{L-1}k_j-1)!}{(N-1)!}. \end{aligned}$$

Finally, the complete expression for the moments of the components of the equivalent noise term are

$$E[n_{eq,m}^{2r}] = N_0 r! \sum_{|\mathbf{k}|=r} \binom{r}{\mathbf{k}} \left[\left(\prod_{i=2}^{L+1} \alpha_{i-1}^{2\sum_{j=L+1-i}^{L-1} k_j} \right) \frac{(N + \sum_{j=L+1-i}^{L-1} k_j - 1)!}{(N-1)!} \right]. \quad (3.17)$$

To conclude, we have obtained the raw moments of the amplitude of elements of the equivalent channel matrix, (3.16), and the elements of the equivalent noise vector, (3.17).

3.4 Equivalent Channel Matrix Distributions

Deriving the exact distribution for the components of the equivalent channel matrix with an arbitrary number of hops has not proven possible. An explicit expression does exist, based on the representation (3.14), but the resulting integral appears extremely complex to solve.

We can make some progress in deriving the distribution as follows. Let $Y = (H_{eq})_{mn}$ and $\alpha_p = \prod_{l=1}^{L-1} \alpha_l$, then

$$p_Y(u) = \int_0^\infty p_{Y|\mathbf{X}}(u) p_{\mathbf{x}}(\mathbf{x}) d\mathbf{x},$$

where $\mathbf{X} = \begin{bmatrix} X_2 & X_3 & \dots & X_L \end{bmatrix}$ and $\mathbf{x} = \begin{bmatrix} x_2 & x_3 & \dots & x_L \end{bmatrix}$. Using the substitution, $w = \prod_{l=2}^{L} X_l$, $p_{Y|\mathbf{X}}(u)$ is the density of a ZMCSCG variable with variance $\frac{\alpha_p^2 w}{2^{L-1}}$ and is given by [21] as

$$\frac{2^{L-1}}{\pi \alpha_p^2 w} \exp\left(\frac{-2^{L-1}|u|^2}{\alpha_p^2 w} \right).$$

It can be seen that the probability density of $(H_{eq})_{mn}$ only depends on its amplitude. This means that the phase of this variable is uniformly distributed, as is the case in a SISO or single hop system. $p_{\mathbf{x}}(\mathbf{x})$ is the joint distribution of a set of i.i.d standard chi square variables with $2N$ degrees of freedom, $X_l, l \in \{2, 3, \dots, L\}$. The density of a chi-square variable with $2N$ degrees of freedom is given by [21, Chap. 18] as $p_{X_l}(x) = \frac{x^{N-1}}{2^N (N-1)!} \exp\left(\frac{-x}{2}\right)$. Hence

$$\begin{aligned} p_Y(u) &= \int_0^\infty \frac{2^{L-1}}{\pi\alpha_p^2 w} \exp\left(\frac{-2^{L-1}|u|^2}{\alpha_p^2 w}\right) \prod_{k=1}^{L-1} \frac{x_k^{N-1}}{2^N(N-1)!} \exp\left(\frac{-x_k}{2}\right) d\mathbf{x}, \\ &= \int_0^\infty \frac{2^{L-1}}{\pi\alpha_p^2 w} \exp\left(\frac{-2^{L-1}|u|^2}{\alpha_p^2 w}\right) \frac{w^{N-1}}{(2^N(N-1)!)^{L-1}} \exp\left(\frac{-\sum_2^L x_k}{2}\right) d\omega. \end{aligned}$$

While this general form for the PDF has not been solved, a solution is obtainable for the two hop case. Here, the integral becomes

$$\begin{aligned} p_Y(u) &= \int_0^\infty \frac{2}{\pi\alpha_1^2 x_2} exp\left(\frac{-2|u|^2}{\alpha_1^2 x_2}\right) \frac{x_2^{N-1}}{2^N(N-1)!} \exp\left(\frac{-x_2}{2}\right) dx_2 \\ &= \frac{2}{\pi\alpha_1^2 2^N(N-1)!} \int_0^\infty x_2^{N-2} \exp(\frac{-2|u|^2}{\alpha_1^2 x_2}) \exp\left(\frac{-x_2}{2}\right) dx_2. \end{aligned}$$

A result for this integral is available [27] in the form

$$\int_0^\infty x^{\alpha-1} \exp\left(\frac{-\beta}{x}\right) \exp\left(-\gamma x\right) = 2\left(\frac{\beta}{\gamma}\right)^{\frac{\alpha}{2}} K_\alpha(2\sqrt{\gamma\beta}). \tag{3.18}$$

In our integral, $\alpha = N-1$, $\beta = \frac{2|u|^2}{\alpha_1^2}$ and $\gamma = \frac{1}{2}$. Hence

$$\begin{aligned} p_Y(u) &= \frac{2}{\pi\alpha_1^2 2^N(N-1)!} 2(2\beta)^{\frac{N-1}{2}} K_{N-1}(2\sqrt{\frac{\beta}{2}}) \\ &= \frac{2}{\pi\alpha_1^2 2^N(N-1)!} 2^{\frac{N+1}{2}} \left(\frac{2|u|^2}{\alpha_1^2}\right)^{\frac{N-1}{2}} K_{N-1}\left(2\sqrt{\frac{|u|^2}{\alpha_1^2}}\right) \\ &= \frac{2}{\pi\alpha_1^2 2^N(N-1)!} 2^N \left(\frac{|u|^2}{\alpha_1^2}\right)^{\frac{N-1}{2}} K_{N-1}\left(2\sqrt{\frac{|u|^2}{\alpha_1^2}}\right) \\ &= \frac{2}{\pi\alpha_1^{N+1}(N-1)!} |u|^{N-1} K_{N-1}\left(\frac{2|u|}{\alpha_1}\right). \end{aligned} \tag{3.19}$$

In (3.19) Y takes complex values so this distribution is in fact two dimensional. As the probability depends only on the amplitude of this complex variable, we can use a variable transformation to give a one dimensional probability distribution based on the amplitude. The polar transform of the real and imaginary parts of u will give the desired result. Let

$$\begin{aligned} u &= a + jb, \\ r &= \sqrt{a^2 + b^2}, \\ a &= rcos\theta, \\ b &= rsin\theta. \end{aligned}$$

With these definitions we use standard transform theory to give

$$\begin{aligned} p_{|Y|}(r) &= \int_{-\pi}^{\pi} \frac{2}{\pi(N-1)!} \left(\frac{r}{\alpha_1}\right)^{N-1} K_{N-1}\left(\frac{2r}{\alpha_1}\right) r d\theta \\ &= \frac{4}{\alpha_1^{N+1}(N-1)!} r^N K_{N-1}\left(\frac{2r}{\alpha_1}\right). \end{aligned} \tag{3.20}$$

In the two hop case, joint distributions of the components from a single row of the equivalent channel matrix can also be obtained. For the single output case this means that the joint distribution of the whole equivalent channel vector is available. Let $(\mathbf{H}_{eq})_m = \mathbf{u}$ and $(H_{eq})_{mn} = u_n, n \in \{1, 2, \ldots, N\}$, then the joint PDF of the equivalent channel vector is given by

$$\begin{aligned} p_{(H_{eq})_i}(\mathbf{u}) &= \int_0^{\infty} \prod_{n=1}^{N} p_{z_n|X_2}(u_n) p_{x_2}(x_2) dw \\ &= \int_0^{\infty} \prod_{n=1}^{N} \frac{2}{\pi\alpha_1^2 x_2} \exp\left(\frac{-2|u_n|^2}{\alpha_1^2 x_2}\right) \frac{x_2^{N-1}}{2^N(N-1)!} \exp\left(\frac{-x_2}{2}\right) dx_2 \\ &= \int_0^{\infty} \frac{2^N}{\pi^N \alpha_1^{2N} x_2^N 2^N (N-1)!} \exp\left(\frac{-2\sum_{j=1}^{N}|u_j|^2}{\alpha_1^2 x_2}\right) w^{N-1} \exp\left(\frac{-x_2}{2}\right) dx_2 \\ &= \frac{2^N}{\pi^N \alpha_1^{2N} 2^N (N-1)!} \int_0^{\infty} \exp\left(\frac{-2\sum_{j=1}^{N}|u_j|^2}{\alpha_1^N x_2}\right) w^{-1} \exp\left(\frac{-x_2}{2}\right) dx_2. \end{aligned}$$

Using (3.18) with $\alpha = 0$, $\beta = \frac{2\sum_{j=1}^{N}|u_j|^2}{\alpha_1^2}$ and $\gamma = \frac{1}{2}$ gives

$$\begin{aligned} p_{(H_{eq})_i}(\mathbf{u}) &= \frac{2}{\pi^N \alpha_1^{2N} 2^N (N-1)!} 2\left(2\frac{2\|\mathbf{u}\|^2}{\alpha_1^2}\right)^{\frac{0}{2}} K_0\left(2\sqrt{\frac{\|\mathbf{u}\|^2}{\alpha_1^2}}\right) \\ &= \frac{4}{\pi^N \alpha_1^{2N} 2^N (N-1)!} K_0\left(\frac{2\|\mathbf{u}\|}{\alpha_1}\right). \end{aligned} \tag{3.21}$$

Once again, this density depends only on the amplitudes of the complex variables $u_j, j \in 1, 2, \ldots, N$. Furthermore, it depends on the sum of these amplitudes squared, or the 2-norm of $\mathbf{u}$. From this, we can obtain the distribution of the envelope of the received signal through a variable transformation. This is the hyper-spherical transform, when considering the components of the row of interest as the basis for a cartesian coordinate system. The transform is as follows:

$$
\begin{aligned}
r &= \sqrt{\textstyle\sum_{n=1}^{N}(H_{eq})_{mn}(H_{eq})_{mn}^{\dagger}} \\
&= \sqrt{\textstyle\sum_{n=1}^{N}|(H_{eq})_{mn}|^2} \\
(H_{eq})_{m,1} &= r\sin\theta_1 \\
(H_{eq})_{m,2} &= r\cos\theta_1\sin\theta_2 \\
(H_{eq})_{m,3} &= r\cos\theta_1\cos\theta_2\sin\theta_3 \\
&\vdots \\
(H_{eq})_{m,N} &= r\textstyle\prod_{k=1}^{N-1}\cos\theta_k
\end{aligned}
$$

$$
p_{\|(H_{eq})_i\|}(r) = \frac{4}{\pi 2^N \alpha_1^{2N}(N-1)!} K_0\left(\frac{2r}{\alpha_1}\right) \det\left|\frac{\delta(\mathbf{u})}{\delta(r,\theta)}\right| d\theta. \tag{3.22}
$$

Here $\det\left|\frac{\delta(\mathbf{u})}{\delta(r,\theta)}\right|$ is the determinant of the Jacobian matrix of the hyper-spherical transform.

In summary, we have obtained a distribution for the elements of $\mathbf{H}_{eq}$ in the two hop case, given by (3.19). The distribution of the amplitude of these complex elements is given by (3.20). For the two hop case, a joint distribution of a row of $\mathbf{H}_{eq}$ is also derived, the result given by (3.21). Finally (3.22) gives the distribution of the 2-norm of a row of $\mathbf{H}_{eq}$.

3.5 SNR Distributions

The SNR is a very commonly used parameter for evaluation of system performance. To allow similar evaluation in our system it would be desirable to define an end to end SNR for relay chains. If we consider one receive antenna in isolation, $r_{L,m}$, the channel model can be written in the more familiar form of a simple Rayleigh channel, that is

$$
r = \mathbf{hs} + vn. \tag{3.23}
$$

Equating (3.23) to our expression for $(r_L)_m$ in (3.14), we have $\mathbf{h} = \mathbf{z}_1$ and

$$
v = \frac{\left[\sqrt{N_0 \sum_{l=1}^{L}\prod_{k=l+1}^{L}\alpha_{k-1}^2\frac{X_k}{2}}\right]}{\prod_{l=2}^{L}\alpha_{l-1}\sqrt{\frac{X_l}{2}}}.
$$

Now, the SNR in a Rayleigh channel is defined as $\frac{E[s^\dagger s]}{v^2}$. Hence, in our system we can define an equivalent end to end SNR (SNR_{eq}) as

$$SNR_{eq} = \frac{\prod_{l=2}^{L} \alpha_{l-1}^2 \frac{X_l}{2}}{N_0\left[\sum_{l=1}^{L} \prod_{k=l+1}^{L} \alpha_{k-1}^2 \frac{X_k}{2}\right]} .$$

The sum in the denominator of this expression makes it difficult to deal with algebraically. To avoid this problem, the inverse of this ratio will be looked at instead. This is the equivalent end to end noise to signal ratio (NSR_{eq}) and it can still be used for evaluation of system performance in place of the standard SNR. The NSR_{eq} is defined by

$$\begin{aligned} NSR_{eq} &= \frac{N_0\left[\sum_{l=1}^{L} \prod_{k=l+1}^{L} \alpha_{k-1}^2 \frac{X_k}{2}\right]}{\prod_{l=2}^{L} \alpha_{l-1}^2 \frac{X_l}{2}} \\ &= N_0 \sum_{l=1}^{L} \left[\frac{\prod_{k=l+1}^{L} \alpha_{k-1}^2 \frac{X_k}{2}}{\prod_{l=2}^{L} \alpha_{l-1}^2 \frac{X_l}{2}}\right] \\ &= N_0 \sum_{l=1}^{L} \left[\frac{1}{\prod_{k=l+1}^{L} \alpha_{k-1}^2 \frac{X_k}{2}}\right] . \end{aligned}$$

As the terms in the sum of the expression for NSR are separable, we can define moments for this ratio. For example the mean is given by

$$\begin{aligned} E[NSR_{eq}] &= E\left[N_0 \sum_{l=1}^{L} \left[\frac{1}{\prod_{k=l+1}^{L} \alpha_{k-1}^2 \frac{X_k}{2}}\right]\right] \\ &= N_0 \sum_{l=1}^{L} E\left[\left(\frac{1}{\prod_{k=l+1}^{L} \alpha_{k-1}^2 \frac{X_k}{2}}\right)\right] . \end{aligned} \tag{3.24}$$

It is left to establish the expected value of products of the form $\prod_l \frac{2}{X_l}$. Let $w_l = X_l, l \in \{2, 3, \ldots, L\}$,

$$\begin{aligned} E[\textstyle\prod_l \frac{2}{X_l}] &= \int_0^\infty \prod_l \frac{2}{w_l} \prod_l \frac{w_l^{N-1}}{2^N(N-1)!} \exp\left(\frac{-w_l}{2}\right) d\mathbf{w} \\ &= \prod_l \int_0^\infty \frac{w_l^{N-2}}{2^{N-1}(N-1)!} \exp\left(\frac{-w_l}{2}\right) d\mathbf{w}. \end{aligned}$$

A result for this integral is given in [27] in the form $\int_0^\infty x^\alpha \exp(-\beta x) = \alpha! \beta^{-\alpha-1}$. Here, $\alpha = N - 2$ and $\beta = \frac{1}{2}$, so that

$$\begin{aligned} E[\textstyle\prod \frac{1}{X_l^2}] &= \prod_l \frac{1}{2^{N-1}(N-1)!} (N-2)! \left(\frac{1}{2}\right)^{-(N-2)-1} \\ &= \prod_l \frac{1}{2^{N-1}(N-1)!} (N-2)! 2^{N-1} \\ &= \prod_l \frac{1}{N-1}. \end{aligned}$$

Substituting this result into (3.24) gives

$$E[NSR_{eq}] = N_0 \sum_{l=1}^{L} \prod_{k=l}^{L-1} \frac{1}{\alpha_k^2} \left(\frac{1}{N-1} \right)^{l-1}.$$

We show the effect of α on NSR_{eq} in Fig. 3.2.

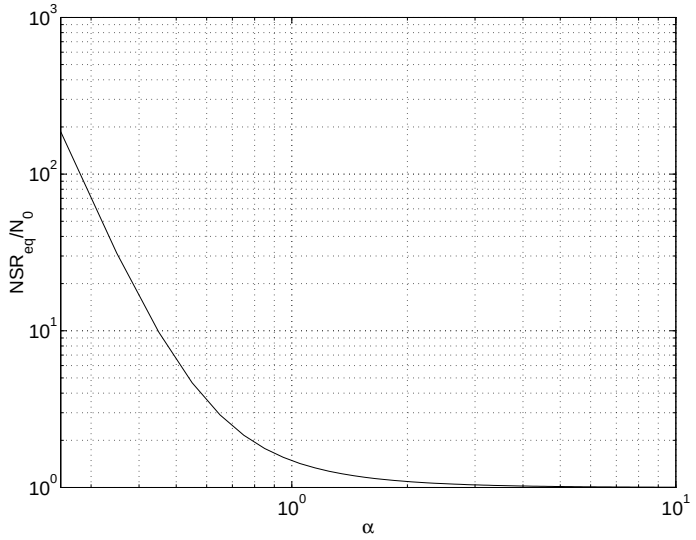

Figure 3.2: $E[NSR_{eq}]$ for different values of α, N=4, L=4

The expressions for higher order moments become more complex. Again we will use the multinomial notation as in Sec. 3.3. Let $Xp_i = \prod_{l=i+1}^{L} \alpha_{l-1}^2 \frac{X_l}{2}$ then,

$$\begin{aligned} E[NSR_{eq}^r] &= E\left[N_0 \left(\sum_{l=1}^{L} \left[\frac{1}{\prod_{k=l+1}^{L} \alpha_{k-1}^2 \frac{X_k}{2}} \right] \right)^r \right] \\ &= N_0 \sum_{|\mathbf{k}|=r} \binom{r}{\mathbf{k}} E\left[\prod_{i=1}^{L} \frac{1}{Xp_i^{k_i}} \right]. \end{aligned}$$

Using the fact that $\prod_{i=1}^{L} Xp_{i+1}^{k_i} = \prod_{i=2}^{L+1} \left(\alpha_{i-1} \frac{X_i}{2} \right)^{\sum_{j=L+1-i}^{L-1} k_j}$ gives,

$$E[NSR_{eq}^r] = N_0 \sum_{|\mathbf{k}|=r} \binom{r}{\mathbf{k}} \prod_{i=2}^{L+1} E\left[\frac{1}{\left(\alpha_{i-1} \frac{X_i}{2} \right)^{\sum_{j=L+1-i}^{L-1} k_j}} \right].$$

It remains to evaluate the expected values $E\left[\frac{1}{\left(\frac{X_i}{2} \right)^{\sum_{j=L+1-i}^{L-1} k_j}} \right]$. Again, let $w_l = X_l, l \in \{2, 3, \ldots, L\}$,

$$\begin{aligned} E\left[\left(\frac{2}{X_l}\right)^k\right] &= \int_0^\infty \left(\frac{2}{w_l}\right)^k \frac{w_l^{N-1}}{2^N(N-1)!}\exp\left(\frac{-w_l}{2}\right) dw_l \\ &= \int_0^\infty \frac{w_l^{N-1-k}}{2^{N-k}(N-1)!}\exp\left(\frac{-w_l}{2}\right) dw_l \\ &= \frac{1}{2^{N-k}(N-1)!}(N-1-k)!\left(\frac{1}{2}\right)^{-(N-1-k)-1} \\ &= \frac{(N-1-k)!}{(N-1)!}. \end{aligned}$$

Finally, we have the general moments as

$$\begin{aligned} E[NSR_{eq}^r] &= N_0 \sum_{|\mathbf{k}|=r} \frac{r!}{\prod_{l=1}^L k_l!}\left(\prod_{i=2}^{L+1} \alpha_{i-1}^{\sum_{j=L+1-i}^{L-1} k_j}\right)\frac{(N-1-\sum_{j=L+1-i}^{L-1} k_j)!}{(N-1)!} \\ &= N_0 r! \sum_{|\mathbf{k}|=r}\left(\prod_{i=2}^{L+1} \alpha_{i-1}^{\sum_{j=L+1-i}^{L-1} k_j}\right)\frac{(N-1-\sum_{j=L+1-i}^{L-1} k_j)!}{k_{i-1}!(N-1)!}. \end{aligned} \tag{3.25}$$

This section defines an end to end SNR, SNR_{eq}, in a similar fashion to standard fading channels. We go on to derive the moments of the inverse of SNR_{eq}, defined as NSR_{eq}. The expression for these moments is given by (3.25).

3.6 Relay Amplification

So far the amplification factors, $\alpha_l, 1 < l < L-1$, have been left arbitrary. Here we consider a specific relaying scheme, defining the values of the amplification factors, and present some properties of the resulting end to end channel.

3.6.1 Fixed Relay Amplification

In a general system it would seem appropriate that $E[\mathbf{s}_{l+1}^\dagger \mathbf{s}_{l+1}] \simeq E[\mathbf{s}_l^\dagger \mathbf{s}_l], l \in \{1, 2, \ldots, L\}$. Consider a system with M transmit antennas. Here, the expected received power can be given by

$$\begin{aligned} E[|r_{lm}|^2] &= E[|((\mathbf{H}_l)_m \mathbf{s}_l + n_{l,m}|^2] \\ &= E[\left(\sum_{n=1}^M |(H_l)_{mn}|^2 |s_{l,n}|^2\right) + (\mathbf{H}_l)_m \mathbf{s}_l n_{l,m}^\dagger + (\mathbf{H}_l)_m^\dagger \mathbf{s}_l^\dagger n_{l,m} + |n_{l,m}|^2] \\ &= \left(\sum_{n=1}^M E[|(H_l)_{mn}|^2] E[|s_{l,n}|^2]\right) + E[(\mathbf{H}_l)_m \mathbf{s}_l n_{l,m}^\dagger] \\ &+ E[(\mathbf{H}_l)_m^\dagger \mathbf{s}_1^\dagger n_{l,m}] + E[|n_{l,m}|^2]. \end{aligned}$$

As n_{lm} is an independent Gaussian variable, $E[(\mathbf{H}_1)_m \mathbf{s}_1 n_{lm}] = 0$,

$$\begin{aligned} E[|r_{lm}|^2] &= \textstyle\sum_{n=1}^{M} E[|s_{l,n}|^2] + N_0 \\ &= E[\mathbf{s}_l^\dagger \mathbf{s}_l] + N_0. \end{aligned}$$

Let $E[\mathbf{s}_{l+1}^\dagger \mathbf{s}_{l+1}] = E[\mathbf{s}_l^\dagger \mathbf{s}_l]$, then it follows, as $E[\mathbf{s}_{l+1}^\dagger \mathbf{s}_{l+1}] = M\alpha^2 E[|r_{lm}|^2]$, so that

$$\begin{aligned} \alpha &= \sqrt{\frac{E[\mathbf{s}_{l+1}^\dagger \mathbf{s}_{l+1}]}{M(E[[\mathbf{s}_l^\dagger \mathbf{s}_l]]+N_0)}} \\ &= \sqrt{\tfrac{1}{M(1+N_0)}}. \end{aligned}$$

Using this value for α_l as a constant across all receive antennas and relay nodes, the system has the following properties:

$$\mathbf{H}_{eq} = \sqrt{\frac{1}{M(1+N_0)}}^{L-1} \prod_{l=1}^{L} \mathbf{H}_l,$$

$$\mathbf{n}_{eq} = \sum_{l=1}^{L} \sqrt{\frac{1}{M(1+N_0)}}^{L-l} \prod_{k=l+1}^{L} \mathbf{H}_k \mathbf{n}_l.$$

These results lead to the follow simplified distributions as in Sec. 3.1,

$$(\mathbf{H}_{eq})_m = \sqrt{\frac{1}{M(1+N_0)}}^{L-1} \prod_{l=2}^{L} \sqrt{\frac{\mathbf{X}_l}{2}} \mathbf{z}_1,$$

$$\begin{aligned} \mathbf{n}_{eq,m} &= \textstyle\sum_{l=1}^{L} \left(\sqrt{\frac{1}{M(1+N_0)}}\right)^{L-l} \prod_{k=l+1}^{L} \sqrt{\frac{\mathbf{X}_k}{2}} \tilde{\mathbf{n}}_l \\ &= \left[\sqrt{\textstyle\sum_{l=1}^{L} \left(\frac{1}{M(1+N_0)}\right)^{L-l} \prod_{k=l+1}^{L} \frac{\mathbf{X}_k}{2}}\right] n. \end{aligned}$$

The moments become,

$$\begin{aligned} E[|(H_{eq})_{mn}|^{2r}] &= \left[\textstyle\prod_{l=2}^{L} \alpha_l^{2r}\right] r! \left(\frac{(M+r-1)!}{(M-1)!}\right)^{L-1} \\ &= r! \left(\frac{(M+r-1)!}{(M(1+N_0))^r (M-1)!}\right)^{L-1}, \end{aligned}$$

$$
\begin{aligned}
E[|n_{eq,m}|^{2r}] &= N_0 r! \sum_{|\mathbf{k}|=r} \binom{r}{\mathbf{k}} \left[\prod_{i=2}^{L+1} \alpha_{i-1}^{2\sum_{j=L+1-i}^{L-1} k_j} \left(\frac{(M+\sum_{j=L+1-i}^{L-1} k_j - 1)!}{(M-1)!} \right) \right] \\
&= N_0 r! \sum_{|\mathbf{k}|=r} \binom{r}{\mathbf{k}} \left[\prod_{i=2}^{L+1} \left(\frac{1}{M(1+N_0)} \right)^{\sum_{j=L+1-i}^{L-1} k_j} \left(\frac{(M+\sum_{j=L+1-i}^{L-1} k_j - 1)!}{(M-1)!} \right) \right] \\
&= N_0 r! \sum_{|\mathbf{k}|=r} \binom{r}{\mathbf{k}} \left(\frac{1}{M(1+N_0)} \right)^{\sum_{j=2}^{L} (j-1) k_j} \left[\prod_{i=2}^{L+1} \frac{M+\sum_{j=L+1-i}^{L-1} k_j - 1)!}{(M-1)!} \right].
\end{aligned}
$$

With the amplification factors now defined, we can plot the moments for various system sizes. Figure 3.3 shows the variance of a component of the equivalent channel matrix. As the expected value of this variable is zero, the variance is the second moment, given by

$$
\begin{aligned}
E[|(H_{eq})_{mn}|^2] &= \left(\frac{1}{M(1+N_0)} \right) \left(\frac{M!}{(M-1)!} \right)^{L-1} \\
&= \left(\frac{1}{1+N_0} \right)^{L-1}.
\end{aligned}
$$

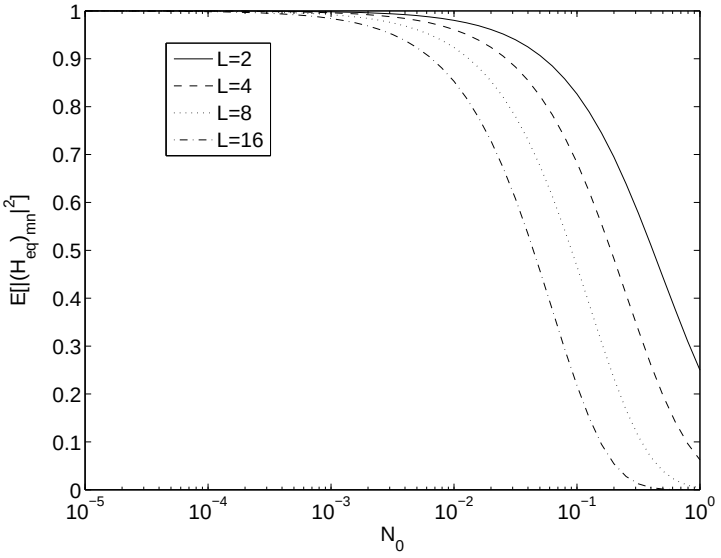

Figure 3.3: Variance of an element of $\mathbf{H}_{eq}$ for a $M \times M$ MIMO system

Figure 3.4 shows the variance of a component of the equivalent noise vector, given by

$$\begin{aligned} E[|n_{eq,m}|^2] &= N_0 \sum_{l=1}^{L} \left(\frac{1}{M(1+N_0)}\right)^{L-l} \left(\frac{M!}{(M-1)!}\right)^{L-l} \\ &= N_0 \sum_{l=1}^{L} \left(\frac{1}{1+N_0}\right)^{L-l}. \end{aligned}$$

Note that $E[|n_{eq,m}|^2]$ is strictly increasing and converges to $1 + N_0$ as $L \to \infty$.

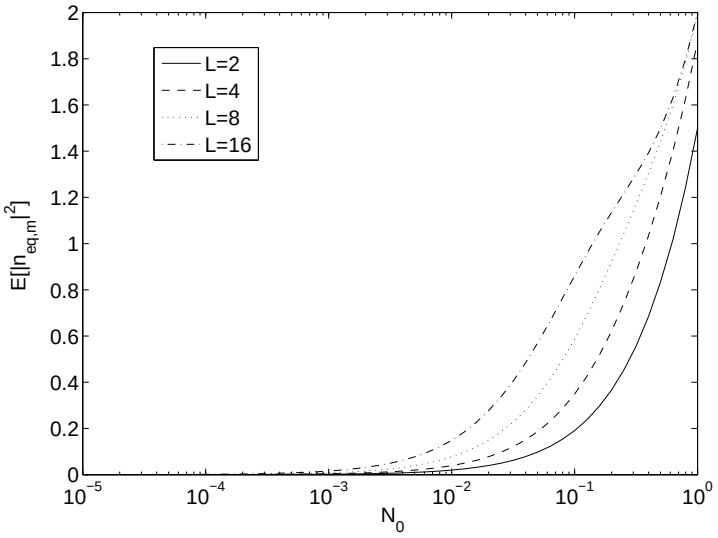

Figure 3.4: Variance of an element of $\mathbf{n}_{eq}$ for a $M \times M$ MIMO system

The distributions of elements of the equivalent channel matrix for a two hop system are:

$$\begin{aligned} p_{(H_{eq})_{mn}}(u) &= \frac{2}{\pi\alpha_1^{M+1}(M-1)!}|u|^{M-1}K_{M-1}\left(\frac{2|u|}{\alpha_1}\right) \\ &= \frac{2(M+N_0)^{\frac{M+1}{2}}}{\pi(M-1)!}|u|^{M-1}K_{M-1}\left(2\sqrt{M+N_0}|u|\right), \\ p_{\|(H_{eq})_{mn}\|}(r) &= \frac{4}{\alpha_1^{M+1}(M-1)!}r^M K_{M-1}\left(\frac{2r}{\alpha_1}\right) \\ &= \frac{4(M(1+N_0))^{\frac{M+1}{2}}}{(M-1)!}r^M K_{M-1}\left(2\sqrt{M(1+N_0)}r\right). \end{aligned}$$

Figure 3.5 shows the probability density of $\|(H_{eq})_{mn}\|$ for a range of antenna numbers, M.

Relating the system to a single flat Rayleigh channel, $E[NSR_{eq}]$ becomes

$$E[NSR_{eq}] = N_0 \sum_{l=1}^{L} \left(\frac{M(1+N_0)}{M-1}\right)^{l-1}.$$

Values for $E[NSR_{eq}]$ are plotted in Figs. 3.6, 3.7 and 3.8 for a range of system sizes. Figures 3.9 and 3.10 show the cumulative density of NSR_{eq} for a SNR of $20dB$.

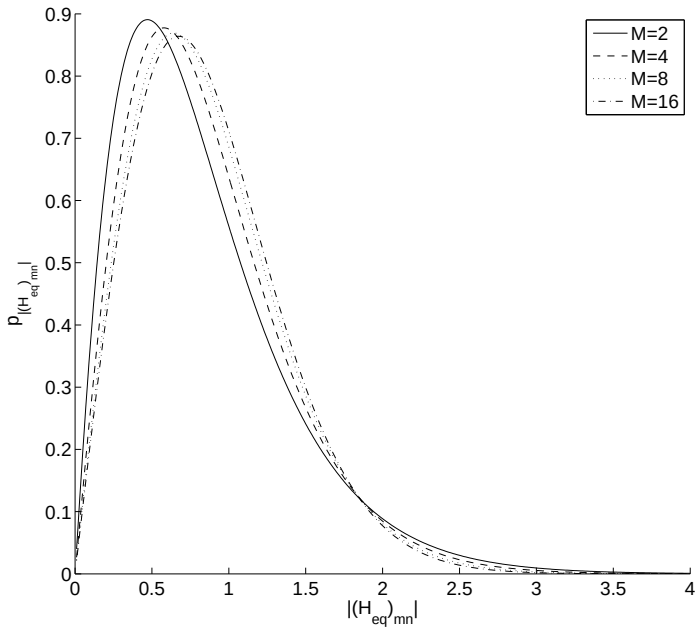

Figure 3.5: Probability density function of $|(H_{eq})_{mn}|$ with $N_0 = 0$

3.7 Eigenvalues

The eigenvalues of the channel matrix are essential indicators of many measures of system performance, including the capacity of a communication system. For the multi-hop relay system the channel matrix is too complex for the distribution of its eigenvalues to be calculated analytically. Therefore, we characterize the distribution of the eigenvalues empirically. As the eigenvalues give the scaling factor that the channel applies to an eigenvector, they provide a relationship between transmitted and received power.

3.7.1 Eigenvalue Decomposition

Any matrix $\mathbf{M}$ can be represented by its singular value decomposition (SVD) as $\mathbf{M} = \mathbf{U}\mathbf{\Lambda}\mathbf{V}^{\dagger}$. Here, $\mathbf{U}$ and $\mathbf{V}$ are unitary matrices and $\mathbf{\Lambda}$ is a diagonal matrix whose entries are the eigenvalues of $\mathbf{M}^{\dagger}\mathbf{M}$. The SVD is defined such that $\mathbf{M}\mathbf{V}_n = \mathbf{\Lambda}_{nn}\mathbf{U}_n$. Using this, we can define the information carrying part of the received signal, $\hat{\mathbf{r}}_L$, as

$$\mathbf{U}\mathbf{\Lambda}\mathbf{V}^{\dagger}\mathbf{s}_1,$$

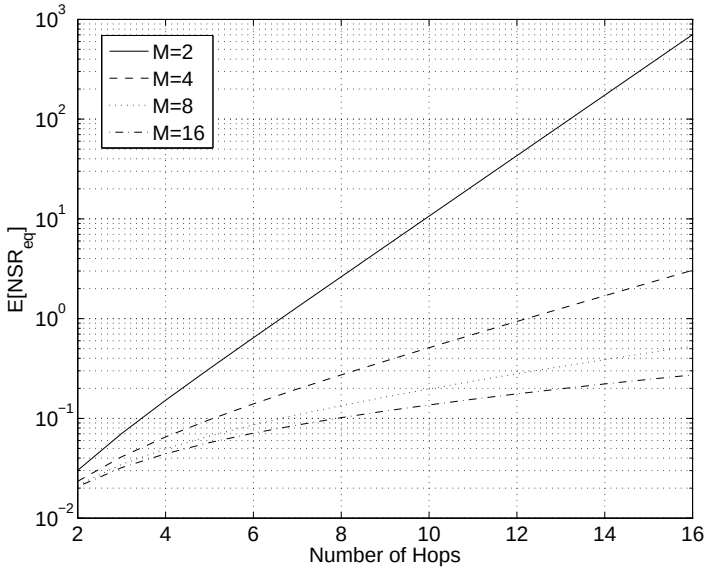

Figure 3.6: Plot of expected end to end noise to signal ratios with a SNR of 10^2

where $\mathbf{H}_{eq} = \mathbf{U}\mathbf{\Lambda}\mathbf{V}^{\dagger}$. The power of the information carrying component of the received signal can then be given by

$$\begin{aligned} E[\hat{\mathbf{r}}_L^{\dagger}\hat{\mathbf{r}}_L] &= E[\mathbf{s}_1^{\dagger}\mathbf{V}\mathbf{\Lambda}^{\dagger}\mathbf{U}^{\dagger}\mathbf{U}\mathbf{\Lambda}\mathbf{V}^{\dagger}\mathbf{s}_1] \\ &= E[\mathbf{s}_1^{\dagger}\mathbf{V}\mathbf{\Lambda}^{\dagger}\mathbf{\Lambda}\mathbf{V}^{\dagger}\mathbf{s}_1]. \end{aligned} \tag{3.26}$$

As $\mathbf{\Lambda}$ is a diagonal matrix, (3.26) can be rearranged to give

$$\sum_{n=1}^{N} |\lambda_n|^2 (\mathbf{s}_1^{\dagger}\mathbf{V})_n (\mathbf{V}^{\dagger}\mathbf{s}_1)_n.$$

Also, as $\mathbf{V}$ is an orthonormal basis for $\mathbb{C}^N$

$$E[\mathbf{s}_1^{\dagger}\mathbf{s}_1] = \sum_{n=1}^{N} (\mathbf{s}_1^{\dagger}\mathbf{V})_n (\mathbf{V}^{\dagger}\mathbf{s}_1)_n.$$

We can now establish a bound on $E[\hat{\mathbf{r}}_L^{\dagger}\hat{\mathbf{r}}_L]$ given by

$$min\{|\lambda_n|^2\}E[s_1^2] \leq E[\hat{\mathbf{r}}_L^{\dagger}\hat{\mathbf{r}}_L] \leq max\{|\lambda_n|^2\}E[s_1^2], n \in \{1, 2, \ldots, N\}.$$

Here we look at the eigenvalues of multi-hop amplify and forward relay links in flat Rayleigh environments. That is the eigenvalues of products of complex Gaussian matrices with a scaling factor applied,

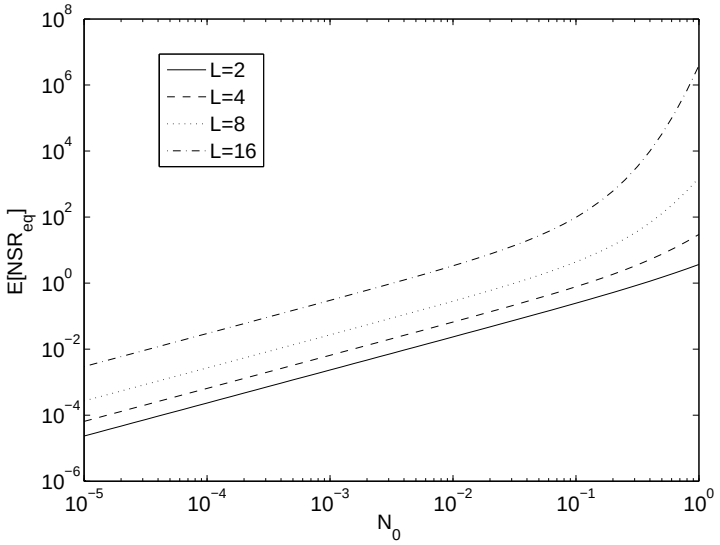

Figure 3.7: Plot of expected end to end noise to signal ratios for a 4×4 MIMO system

$$\prod_{l=1}^{L} \alpha H_l,$$

where $H_l, l \in 1, 2, \ldots, L$ is a $N \times N$ matrix of i.i.d $\mathbb{C}N(0,1)$ variables with zero mean and unit variance, $\alpha = \sqrt{\frac{1}{N}}$. The channel matrix, being of rank N, will have N eigenvalues. Figure 3.11 shows the average eigenvalue for all N eigenvectors, for different values of N and the number of hops.

We can see that the average magnitude of the eigenvalues decreases as the number of relay nodes increases, implying a drop in capacity with an increasing number of hops as would be expected. Less intuitive is the fact that the eigenvalues become smaller as the dimension of the antenna array, M, is increased also. This trend suggests that the fixed gain relays are not optimal for this system which is no surprise. To further investigate what is happening as the system dimension increases we can look at the average values of individual eigenvalues. Figure 3.12 shows these values for a system with 8 hops.

In Fig 3.12 the individual eigenvalues are arranged along the x axis from smallest to largest. When considering the area under the curves it is apparent the average magnitude of all of the eigenvalues decreases. This is consistent with Fig. 3.11. With

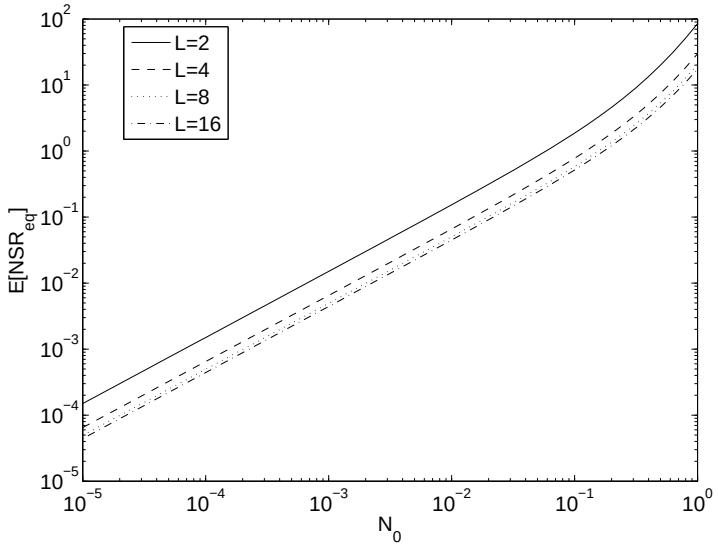

Figure 3.8: Plot of expected end to end noise to signal ratios for a four hop system

the received power bounded by the maximum and minimum eigenvalues it can be seen, for signals carried on the weaker eigenchannels, that the received power could tend to zero as the dimension increases. However, if the transmitter has knowledge of the channel eigenvectors the potential capacity of the channel could be retained with the maximum eigenvalue, by using this eigenvector to carry the transmission symbol.

3.8 Channel Approximations

Here we consider approximations to the distributions in the system. Note that one needs to be careful in considering the use of such approximations, as the dependencies in the system cannot be ignored. Assuming $\alpha_l = \frac{1}{M(1+N_0)}$, first we will look at the distribution of $(H_{eq})_{mn}$ using the representation given by $\prod_{l=2}^{L} \sqrt{\frac{1}{M(1+N_0)} \frac{X_l}{2}} z$. From this representation, we can see that $(H_{eq})_{mn}$ is distributed as a $\mathbb{C}N(0, \prod_{l=2}^{L} \frac{1}{M(1+N_0)} \frac{X_l}{2})$ variable. Hence, the phase of $(H_{eq})_{mn}$ is uniformly distributed on the interval $[-\pi, \pi)$. Figure 3.13 shows the results of fitting some standard distributions to the distribution of $|(H_{eq})_{mn}|$. Two distributions, the Gamma ([21] Chap. 17) and Generalized Extreme Value (GEV) ([21] Chap. 22), were found to give a close fit. A Rayleigh distribution is also shown, to illustrate how the distribution differs from

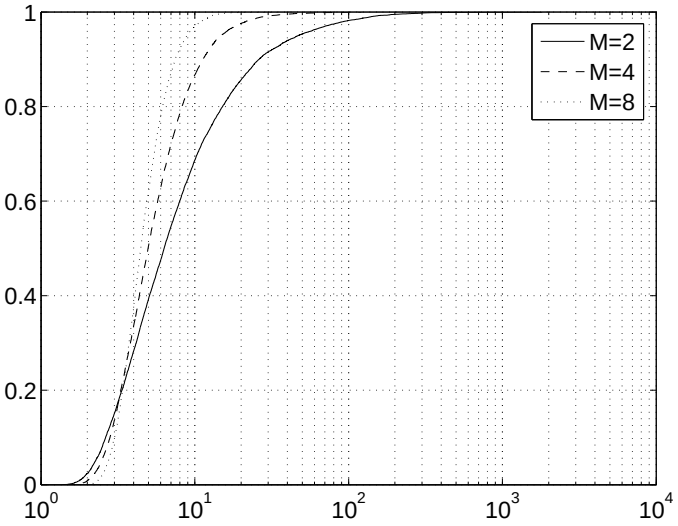

Figure 3.9: Cumulative density of NSR_{eq} for a four hop system with a SNR of 10^{-2}

a ZMCSCG.

Next consider $n_{eq,m}$, which has the same distribution as $\sqrt{\sum_{l=1}^{L}\prod_{k=l+1}^{L}\frac{1}{M(1+N_0)}\frac{X_k}{2}}n$. From this representation, we can see that $n_{eq,m}$ is distributed as

$$\mathbb{C}N(0,\sum_{l=1}^{L}\prod_{k=l+1}^{L}\frac{1}{M(1+N_0)}\frac{X_k}{2}),$$

hence the phase of $n_{eq,m}$ is uniformly distributed on the interval $[-\pi,\pi)$. Figure 3.14 shows the results of fitting some standard distributions to the distribution of $|n_{eq,mn}|$. The GEV distribution was found to give a close fit. A Rayleigh distribution is also shown, to illustrate how the distribution differs from a ZMCSCG.

Finally we look at the distribution of NSR_{eq}. Figure 3.15 shows a possible approximation, the GEV distribution. Once again a Rayleigh distribution is shown for reference.

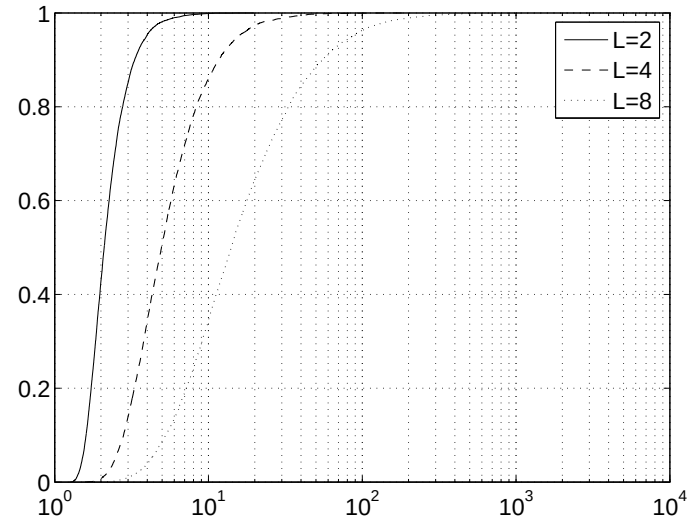

Figure 3.10: Cumulative density of NSR_{eq} for a 4×4 MIMO system with a SNR of 10^{-2}

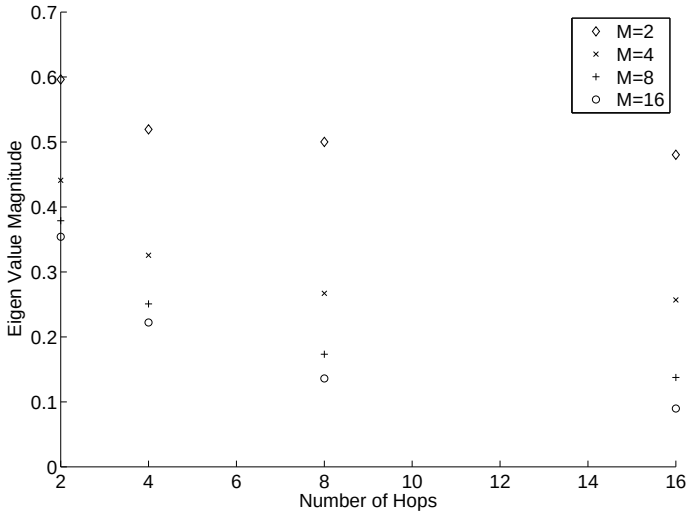

Figure 3.11: Magnitude of the average eigenvalue

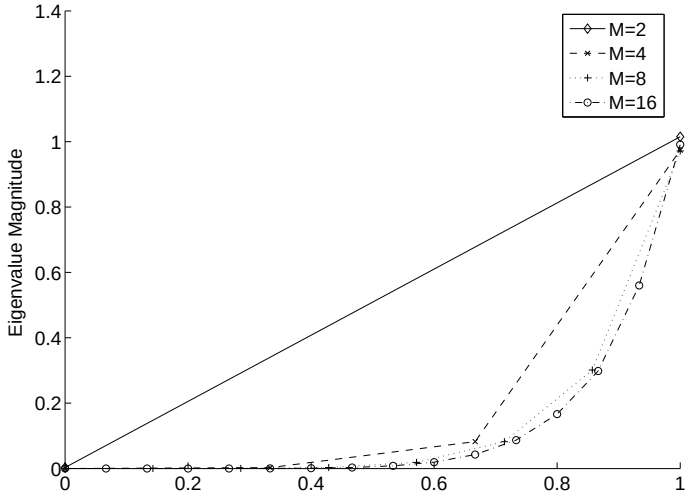

Figure 3.12: Magnitude of the individual eigenvalues for an 8 hop system.

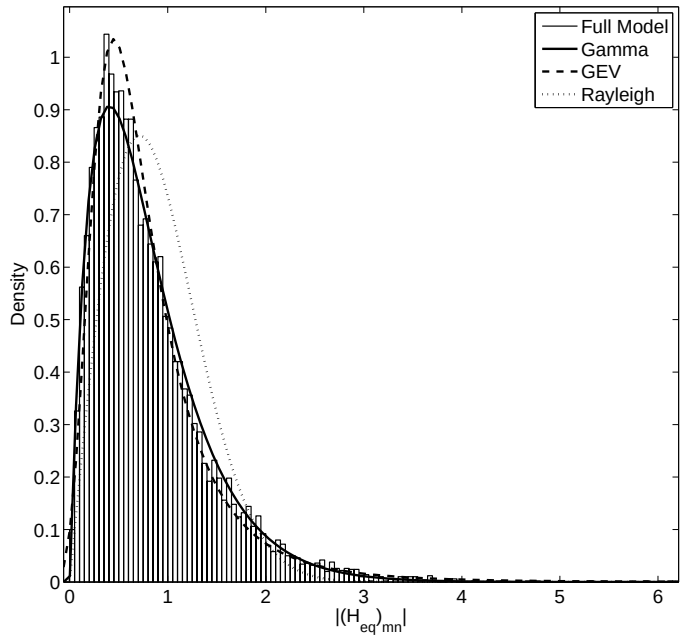

Figure 3.13: PDF of $|(H_{eq})_{mn}|$, for a system where $H = L = 4$ and $N_0 = 10^{-2}$

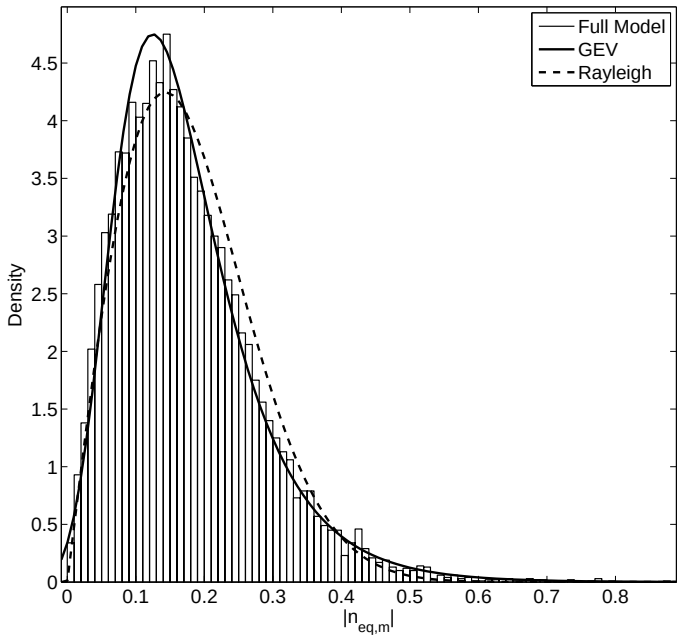

Figure 3.14: PDF of $|n_{eq,mn}|$, for a system where $H = L = 4$ and $N_0 = 10^{-2}$

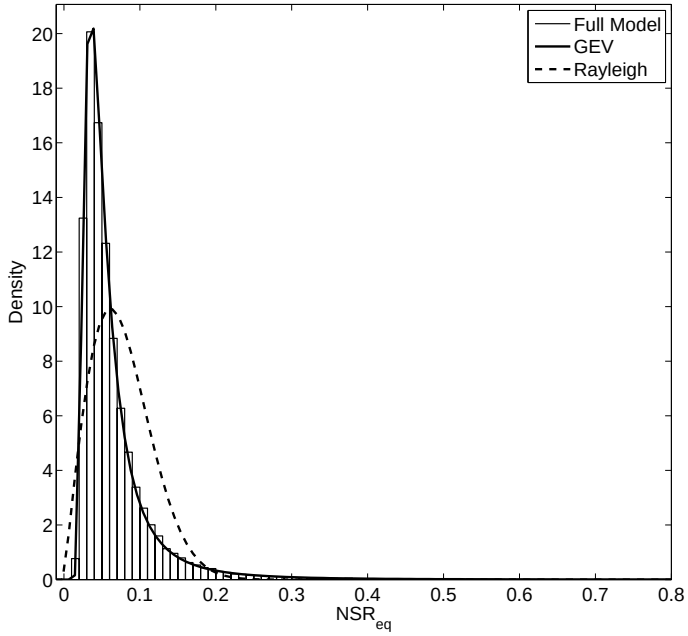

Figure 3.15: PDF of $|NSR_{eq}|$, for a system where $H = L = 4$ and $N_0 = 10^{-2}$

Chapter 4

P25 SISO Simulations

These simulations of a P25 relay chain are intended to facilitate informed system design decisions. We aim to provide as complete an understanding as is possible of the effects of multiple relay hops on the P25 communication protocol. To facilitate this, simulations are run to isolate each cause of communication error, establishing how their effect varies with the number of relays in the link. The simulations include the effects of slow and fast fading (Secs. 4.3 & 4.4), ISI and additive noise. The impact on communication performance by each of these factors is considered before the criterion for the complete system to maintain a given BLER/BER is established (Secs. 4.5 & 4.6).

4.1 Simulation Methodology

This work uses the baseband simulation methodology. This approach ignores the passband phase of the physical system, where the transmitted message is imposed on the carrier signal. The result of this simplification is the assumption of perfect synchronization of the carrier at the transmitter and receiver as well as perfect channel filters isolating the baseband. Also ignored is the analogue nature of a physical system. This means that issues such as sampling jitter, quantization error, amplifier distortion and internal electrical distortions are not accounted for. As a result, the results give an upper bound on what is physically realizable.

As we are simulating a system modeled using random processes, the desired result is the expected performance over an extended period of time. This is not the same as the performance at a given instance. Obtaining these expected values from the simulations requires a different approach depending on which parts of the model are considered to be variable in a given scenario. In slow fading conditions, the change in the channel properties does not disturb the relationship between adjacent symbols, but does vary the received power over the duration of transmission. Thus, to give a representation of average performance in the presence of slow fading a large number of channel realizations need to be simulated. The performance metrics from each realization are averaged to give the final result. To account for fast fading conditions the possibility of errors generated from the channel varying between adjacent symbols needs to be considered. Obtaining the average performance in this situation requires a long sequence of symbols to be simulated, with a correlated random process representing the channel.

4.2 Implementation Details

For the source signal, random integers are generated between zero and three. This sequence is up sampled by a factor of ten to account for the difference between the 4.8kHz symbol frequency and the 48kHz integrator used for DPSK modulation. The integers are then mapped to the appropriate symbol in the signal constellation as described in Chap. 2. These symbols then dictate the phase change between samples in the baseband signal. The modulated signal is then upsampled again by a factor of ten to allow more accurate modeling of the effects of the propagation channel. If the simulations use the convolution codes, the transmitted message is encoded from the 4.8kHz sample stream before upsampling and modulation. The power of the transmitted signal, $E[|s_1|^2]$, is normalised to be equal to one.

For slow fading simulations, the Rayleigh channel is given by $\frac{1}{\sqrt{2}}(x + jy)$, where x, y are pseudo random real Gaussian variables. In the simulation of a Rayleigh channel for fast fading environments we assume the power spectral density of the channel to be that of the Jakes Doppler spectrum. This is given by

$$S(v) = \frac{1}{\pi f_d \sqrt{1 - \left(\frac{v}{f_d}\right)^2}},\ v \in [-f_d, f_d],$$

where v is the frequency shift relative to the carrier frequency. For values of v outside the interval $[-f_d, f_d]$, $S(v)$ is considered to be zero. To generate a sequence of channel path gains the following steps are taken:

1. A complex, uncorrelated (white) Gaussian process, with zero mean and unit variance is generated in discrete time.

2. This Gaussian process is filtered by a doppler filter with the response, $H(v) = \sqrt{S(v)}$, to give the complex random process z_k.

3. The filter process is interpolated, by a combination of linear and polyphase techniques, to give a sample period consistent with the input signal.

4. Finally z_k is scaled to match the average power of the channel path, giving the sequence of complex path gains, a_k. This scaling is performed differently for Rayleigh and Rician paths.

   Rayleigh Fading:

   $$a_k = \sqrt{E[|a_k|^2]} z_k.$$

   Rician Fading:

   $$a_k = \sqrt{E[|a_k|^2]} \left[\frac{z_k}{\sqrt{K_{rk} + 1}} + \sqrt{\frac{K_{rk}}{K_{rk} + 1}} \exp(j(2\pi f_{d,LOS,k} t + \theta_{LOS,k})) \right].$$

   K_{rk} is the Rician K-factor of the k^{th} path, $f_{d,LOS,k}$ is the Doppler shift of the LOS component of the k^{th} path and $\theta_{LOS,k}$ is the initial phase of the LOS component of the k^{th} path.

To implement the multi-path model the output is given by

$$r_t = \sum_{n=-N_1}^{N_2} g_n s_{t-n},$$

where $\{g_n\}$ is a set of weights given by

$$g_n = \sum_{k=1}^{K} a_k sinc\left(\frac{\tau_k}{T_s} - n\right), \quad -N_1 \leq n \leq N_2. \tag{4.1}$$

In (4.1), T_s is the sample period of the input. $\tau_k, 1 \leq k \leq K$ is the set of path delays, K being the number of paths in the channel model and $a_k, 1 \leq k \leq K$ are the set of time dependent complex path gains of the model. These path gains are uncorrelated. N_1 and N_2 are chosen such that $|g_n|$ is small when n is outside the interval $[-N_1, N_2]$. The path gains, a_k, are generated as outlined above for either the slow or fast fading case.

Relaying is performed in one of the following ways depending on the specific protocol being modeled. In these descriptions, the subscript l refers to the signal corresponding to the l^{th} relay.

Amplify and Forward (AF) The received signal, r_l, is multiplied by a constant real scalar to give the transmitted signal, s_{l+1}. The scaling factor, α_l, is

$$\sqrt{\frac{1}{E[|s_l|^2]E[|h|^2] + N_0}}$$

, as this results in the average transmit power for all relays being equal to the originally transmitted power. As $E[|s_l|^2] = 1$ and $E[|h|^2] = 1$, $\alpha_l = \sqrt{\frac{1}{1+N_0}}$.

Phase Forward (PF) The amplitude of the received signal, r_l, is set to one to give the transmitted signal, s_{l+1}. This is achieved by taking the phase from r_l and regenerating a complex signal of amplitude one with the same phase, $s_{l+1} = \exp(\arg(r_l))$.

Detect and Regenerate (DetR) Symbol estimation is performed at each relay and the transmitted signal is generated from these estimates. The symbol estimates are obtained by first demodulating the received signal, r_l. This is done by taking the phase difference between two consecutive samples $m_t = r_{lt} r_{lt-1}^{\dagger}$, where m_t is the demodulated signal at sample time t and r_{lt} is the received signal at sample time t. Due to channel distortion, the demodulated signal does not necessarily correspond to a valid symbol. To obtain the most likely transmitted symbol from the noisy signal received, each sample of m_t can be mapped to the

valid symbol with the smallest phase difference. The symbol estimates, $\tilde{m}_t$, are the values of $m' \in \{-3, -1, 1, 3\}$ that minimize

$$\left| \arg \left(r_{it} r_{i(t-1)}^{\dagger} \exp \left(\frac{-j\pi m'}{4} \right) \right) \right|.$$

Decode and Regenerate (DecR) This protocol applies to transmitted signals in which the information has been encoded using the interleaving and convolution codes described in the P25 specification [24]. Symbol estimation on the received signal is performed as for the DetR protocol. Then the symbol estimates, $\tilde{m}$, are deinterleaved and used to estimate the original message bits via a Viterbi algorithm. Once a message estimate has been obtained it is interleaved and encoded again, giving the transmitted signal, s_{l+1}. For full details of the coding algorithms see Chap. 6.

The noise is simulated using the same pseudo random Gaussian generator as used for the flat Rayleigh channel. Two Gaussian numbers are used to model complex noise in the form $n_r + jn_i$. This noise term is scaled to give the desired average SNR. As $E[|s_1|^2] = 1$, the appropriate scaling term is $\sqrt{\frac{2}{SNR}}$.

The signal is demodulated at the receiver by mapping the change in phase of the received signal between samples to the symbol constellation as given in Chap. 2. Before demodulation, the received signal is downsampled by a factor of ten, to a sample rate of 48kHz. After the signal is demodulated it is downsampled by a further factor of ten to a 4.8kHz sample rate. This is the estimate of the transmitted message. If the message has been encoded, it is decoded using a Viterbi algorithm.

4.3 Slow Fading Relay Channels

The first set of simulations looks at the effects of slow fading environments. In this case the Doppler spread in the channel models is set to zero. The physical situation this would approximate is an environment where there is very little movement of radio nodes or surrounding scattering objects. In these simulations, errors are introduced from additive noise and ISI. Average BER rates are presented based on

a large number of random channel realizations. Enough realizations were included to provide smooth results. This set of simulations is run with a number of hops varying between 2 and 16 and the average received SNR is constant across all radio nodes at 30dB. There is no particular reason this value is chosen and Figs. 4.6 - 4.8 look at how BER changes with SNR. In the results presented, the flat Rayleigh channel shows the effects of the fading channel alone while the other environments introduce errors from ISI as well. In addition, the rural environment includes the effects of a LOS path.

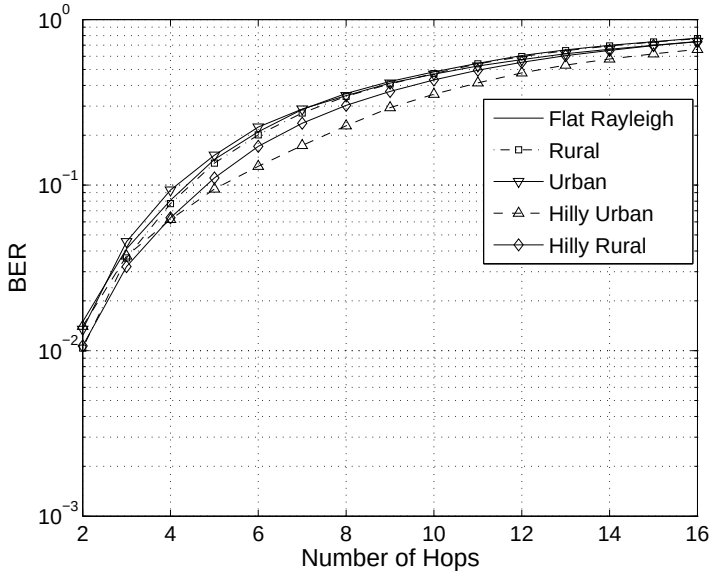

Figure 4.1: BER vs the number of hops for stationary AF relay chains at 30dB SNR. Transmission distance increases with the number of hops.

Results for the AF protocol are shown in Fig. 4.1. Here, the radio environment makes little difference to the results, suggesting that the errors are primarily a result of periods of low instantaneous SNR due to the fading channel. As noise is accumulated per relay node with the same SNR at each node, the total noise power introduced to the system increases linearly with the number of hops. To see how this relates to the SNR at the final receiver we can look at the distributions of signal and noise powers. Figure 4.2 shows the distribution of SNR_{eq} at the final receiver, for systems with various numbers of hops in a flat Rayleigh environment. This distribution can be obtained by taking the ratio of the squares of the signal

and noise components across all the channel realizations, given by:

$$\frac{\alpha^{2L}\prod_{l=1}^{L} h_l^2}{\left(\sum_{l=1}^{L}\prod_{k=l+1}^{L}\alpha h_k n_l\right)^2}.$$

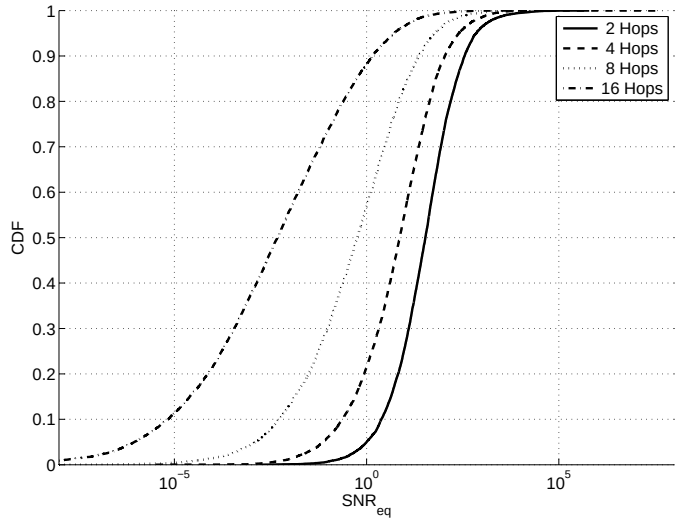

Figure 4.2: CDF of SNR_{eq} for AF relays in flat Rayleigh fading environments

The probability of low SNR increases with the number of hops. In addition to the mean SNR_{eq} decreasing due to increasing total system noise the variance increases, also causing a higher BER. The AF protocol, as used here, would be inappropriate for use in a multi-hop relay system, as clearly its efficiency would be very low.

Figure 4.3 shows that the PF protocol provides substantially improved performance over AF in the rural and flat Rayleigh environments. Note that the rural environment has a narrow delay power profile and LOS. These two environments show how the PF protocol begins to control the fading effects in the presence of multiple relays. Looking at SNR_{eq} for this protocol in the flat Rayleigh environment, Fig. (4.4), it can be seen the variance of the channel is better managed. This provides a smaller variance in SNR_{eq}.

In the other three environments, those with significant delay spreads and the correspondingly higher degree of ISI, the performance is considerably lower. As discussed in Chap. 2, it would be expected for performance to drop in this manner, as the power of the signal is spread in time with increasing relaying hops. PF still

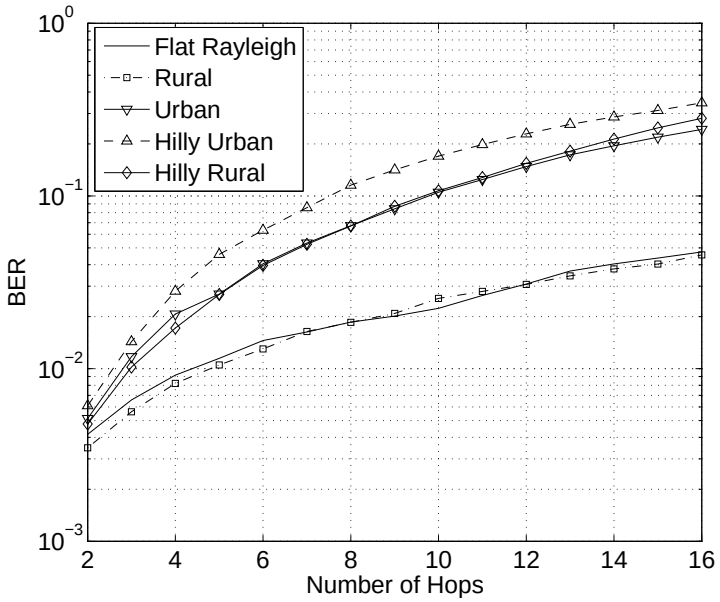

Figure 4.3: BER vs the number of hops for stationary PF relay chains at 30dB SNR. Transmission distance increases with the number of hops.

outperforms AF in these environments, due to its better control of the variance in the fading channel. As this protocol also offers the advantage of easier implementation over AF it would be the obvious choice of the two for a practical system.

In Fig. 4.5 the DetR protocol is considered. The BER performance is consistent in all the modeled radio environments, outperforming PF significantly in the presence of delay spread. This approach degrades more slowly with the number of hops than both AF and PF. The fact that the performance in all the environments is similar suggests that BER is limited chiefly by SNR with this protocol. As the DetR protocol performs symbol estimation and regenerates the signal at each relay, the cascaded effects of the propagation channel are no longer relevant. Each hop in the link can be considered in isolation, albeit with the problem of error propagation now arising. As a result, demodulation does not have to be performed under the severe temporal dispersion conditions experienced at the final receiver when using analogue relaying. It can be seen that this gives a significant advantage over PF relays in reducing ISI. The relevant received SNRs for these relays correspond to only one hop. The distribution of instantaneous SNR in this case is the same as that of single hop systems. As symbol estimation is performed at each relay, it would be

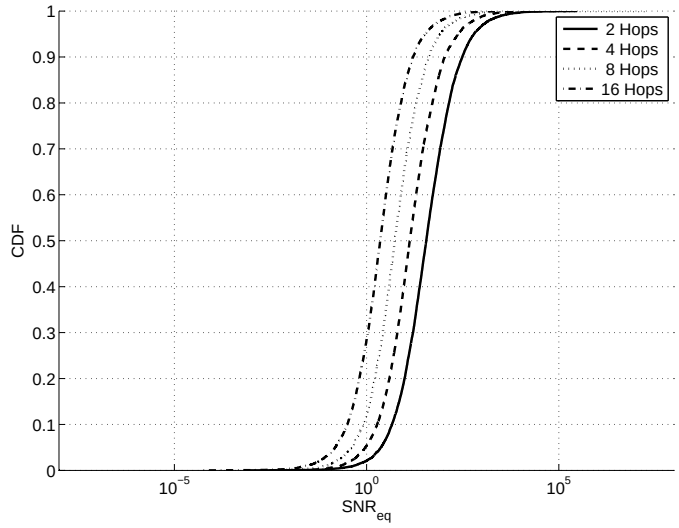

Figure 4.4: CDF of SNR_{eq} for PF relays in flat Rayleigh fading environments

expected that the BER will increase roughly linearly with the number of hops when the BER is low.

4.3.1 SNR Effect on BER

To see how the performance of the system changes with varying noise levels in a slow fading environment, the simulation is repeated. This time, the number of hops is fixed at four and the value of the average SNR at each relay node is varied from 0-50dB.

Comparing Fig. 4.6 with Fig. 4.7 when using AF relays, the BER decreases only slowly with increasing SNR, compared to a system using PF relays. The large amount of variance in received power that occurs when using AF relays means that even as the SNR increases there will be periods of low instantaneous end to end SNR. These will result in a relatively large number of errors. We can see that, contrary to the other results presented, the radio environments with wider power delay profiles provide better BER results than those with narrower power delay profiles at high SNR. This can be attributed to the fact that the environments which spread the signal power over a larger number of paths reduce the probability of periods of deep fades in received power, as this would require all the signal paths to be in a state of

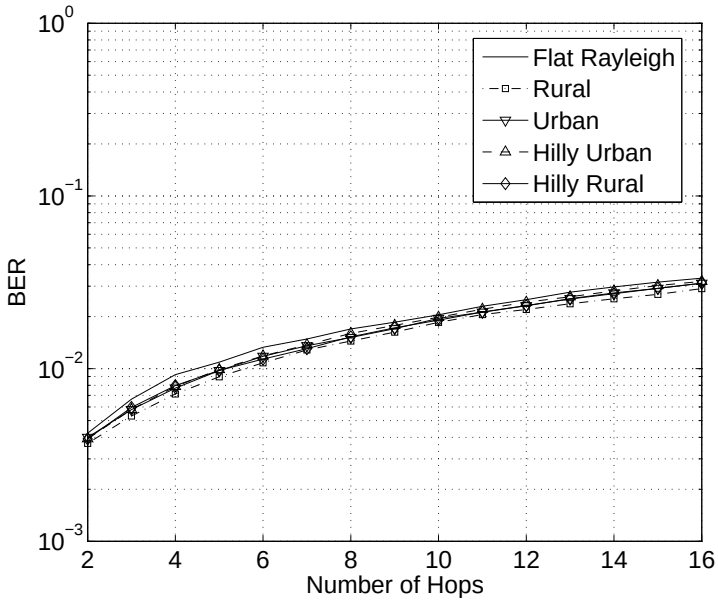

Figure 4.5: BER vs the number of hops for stationary DetR relay chains at 30dB SNR. Transmission distance increases with the number of hops.

deep fade.

The results for the PF protocol are given in Fig. 4.7. As mentioned above, the BER using PF relays improves much faster with increasing SNR than with AF relays, as the likelihood of periods of low instantaneous end to end SNR are reduced. With the PF protocol, increasing SNR shifts the cause of the majority of errors from the fading effect to errors caused by ISI. Hence, unlike the AF protocol, environments with wide power-delay profiles give higher error rates than those with narrower power delay profiles at high SNR. Looking at the Hilly Urban environment, there are similar results for both the AF and PF relays. This suggests that a wide power-delay profile can have as strong an effect on reducing fading errors as relay amplification, at the expense of introducing the ISI problem.

Figure 4.8 shows the results for DetR relays. Here, the decrease in BER with SNR is similar, while being slightly lower, to the flat Rayleigh environment with PF relays. This rate of decrease is retained in all the radio environments modeled, due to the reduction in ISI errors. At high SNR the DetR protocol starts to significantly outperform PF relays in a flat Rayleigh environment. This shows that although the use of PF relays reduces the variance in received power across multiple hops, it still

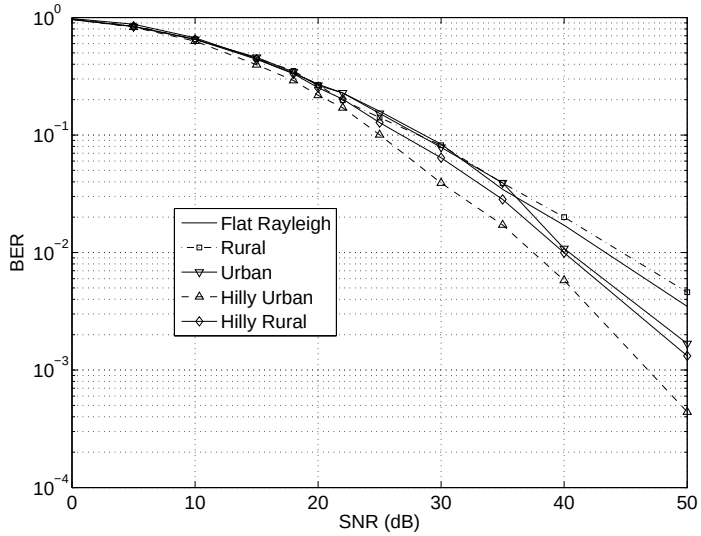

Figure 4.6: BER vs SNR for AF relays

results in a higher channel variance than a single hop.

4.4 Fast Fading Relay Channels

To assess the effects of fast fading channels, relay links were also simulated without added noise. The level of error introduced by the fading channel due to phase distortion in the demodulated signal is therefore established. These simulations use a Doppler spread, f_d, of 78Hz. This is based on a carrier frequency of 800MHz and a 100km/h relative velocity of radio nodes. As the 78Hz doppler spread is applied to each hop in the simulation it does not represent a physically consistent scenario as this would involve all the relay nodes diverging from one another in space. Rather, it is intended to identify the effect of the cascaded channel in fast fading environments. Once again, the flat Rayleigh environment provides a result purely due to the fading channel, while the other environments suffer from multi-path effects. Results for the AF protocol are not presented here, as with no additive noise the amplitude of the signals does not effect the demodulated message. Because the amplitude has no effect, any relay protocols that simply amplifies the signal will be equivalent. This means that the AF and PF protocols will give the same results in these simulations.

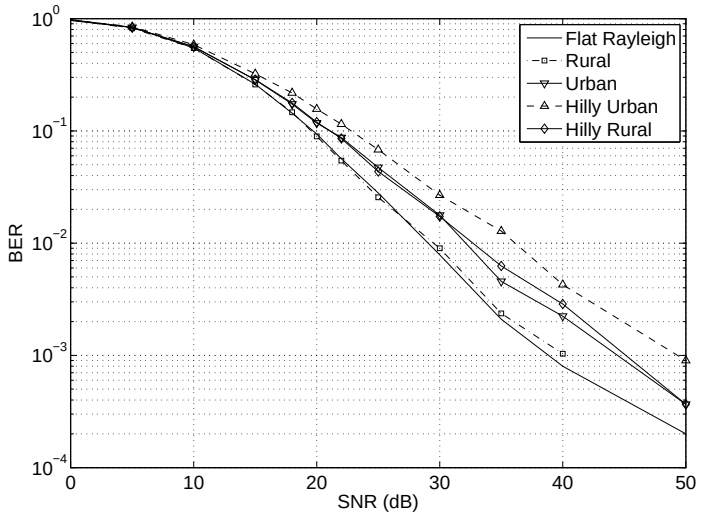

Figure 4.7: BER vs SNR for PF relays

In the absence of noise, the magnitude of the channel gains have no effect on the communication system and any errors introduced are the result of the time varying component of the channel phase and inter symbol interference (ISI). As the transmission system uses differential modulation, errors introduced due to the time varying channel will be related to the ratio of the modulated sample period, 21μs, and the rate of change of the channel gain. It is shown in Chap. 2 that the correlation between successive channel gains can be approximated by $J_0(2\pi \times 78 \times 21 \times 10^{-6})$, which equals 0.99997. With this high degree of correlation between the channel gains, errors due to phase distortion in the channel should prove to be a relatively minor concern. Results for this scenario using PF relays are given in Fig. 4.9. Since the flat Rayleigh environment has only one path it does not introduce any ISI. Any errors result reflects the effect of the time varying channel only. The rural environment has a LOS path, which is unaffected by fading. It also has little ISI and so produces very low error rates. The other three environments produce significantly higher error rates as the number of hops increase. This demonstrates that ISI due to delay spread is a much greater concern in PF relay systems than the time varying nature of the channel when large numbers of relays are employed in a P25 system.

Figure 4.10 shows again the advantage of performing symbol estimation at each relay. With DetR relays, the environments with larger delay spreads do not cause a

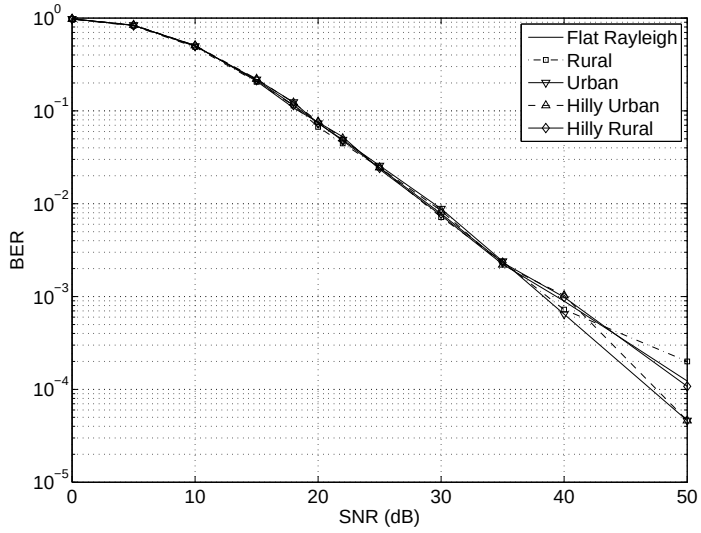

Figure 4.8: BER vs SNR for DetR relays

significant additional increase in BER as the number of relay nodes increases. This suggests that the effects of ISI over a single hop are relatively minor. Again, we would expect the BER to increase roughly linearly with the number of hops while error rate are low. The LOS path in the rural environment once again results in a lower BER. Looking at these results we can see that the limit to the number of relay hops that can be tolerated is much higher than when using analogue relays. Given a high enough SNR, DetR relays could support an extremely large number of relay nodes when using the P25 protocol in these conditions.

4.4.1 The Effect of Doppler Spread on BER

Here we look at the effect of different Doppler spread values on the BER of the system. Figure 4.11 shows the relationship for PF relays in a system consisting of four hops.

As is expected, the BER increases with a higher Doppler spread in the propagation channel. The difference in BER across the radio environments can be attributed to the differing degrees of ISI in the various environments.

The results for a similar system using DetR relays is given in Fig. 4.12. Here we can see, with the lesser degradation due to ISI, that the majority of radio en-

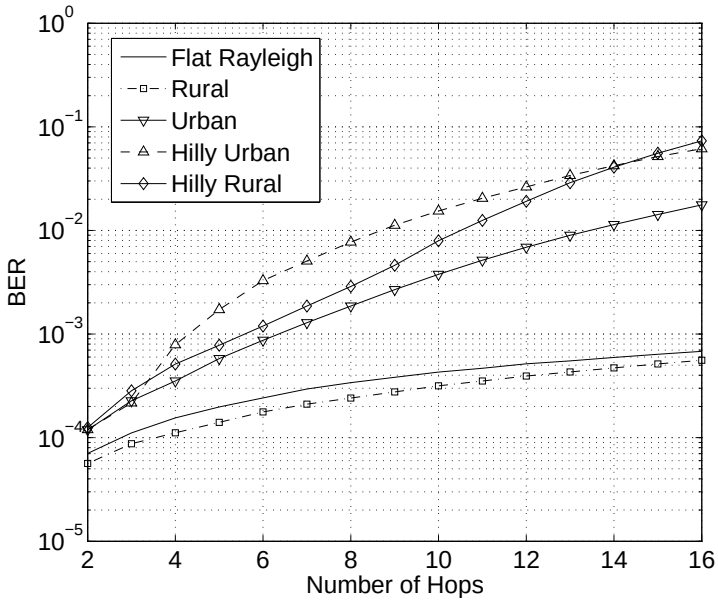

Figure 4.9: BER for PF relays with a fading speed of 100km/h in each link and no additive noise.

vironments produce the same BER. The exception is the rural environment, where the LOS path provides a proportion of the received signal power unaffected by the channel spreading.

4.5 BER Limit

While Secs. 4.3 and 4.4 attempt to isolate the various channel properties, quantifying their individual effects on system performance, we will now look at results for a model of an actual system scenario. The system envisioned consists of two mobile radio nodes, communicating via a series of fixed relay nodes. In terms of our model, slow fading channels are used between relay nodes, with fast fading channels between the transmitter and first relay and the last relay and receiver. The maximum number of relay nodes in a link maintaining a 2% BER is calculated for a range of SNR values. In this simulation the relative speed between transmitter/receiver and the relay nodes is 100km/h, with an 800Mhz carrier frequency. The SNR is the same at each relay, so this simulation represents a transmission distance which increases linearly with the number of hops.

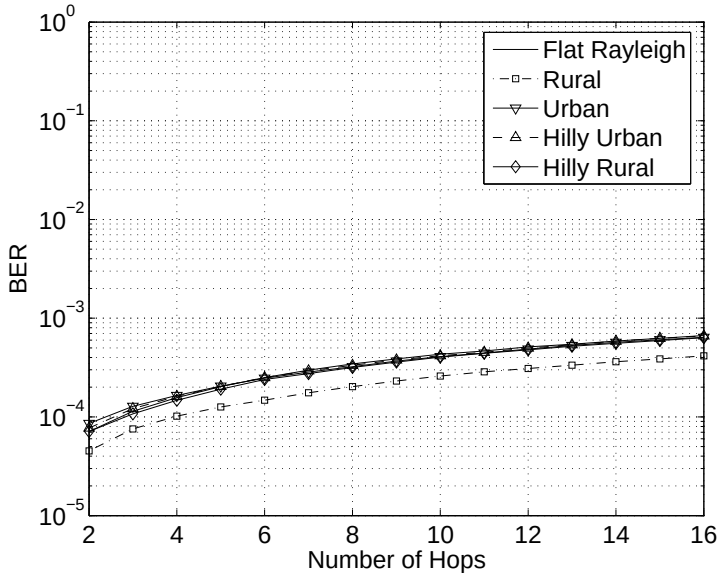

Figure 4.10: BER for DetR relays with a fading speed of 100km/h in each link and no additive noise.

As would be expected, given the results shown in Fig. 4.1, Fig. 4.13 shows that AF relays are not appropriate for multi-hop transmissions. Very high SNR values are required to support reliable transmission with multiple relay nodes. This makes the AF approach especially inappropriate for a low power transmission system.

The PF results, shown in Fig. 4.14, are much more promising. In the rural environment, performance can be maintained through multiple relays, without drastically increasing SNR requirements. The other environments prove a problem though. Referring to Fig. 4.9, we can see the reason why the required SNR increases asymptotically with the number of hops. At a certain number of hops, errors due to ISI reach levels near 2%, independently of the received SNR. While this problem could be mitigated using channel equalizers at the receive terminal or relays, the complexity of equalizing relays would be such that any cost and power saving over a digital relay would most likely be undermined. Given these considerations, it would seem that analogue relays should be limited to links with a small number of relays, in anything but rural environments.

As has been seen in Fig. 4.10 and Fig. 4.8, with sufficiently high SNR the DetR protocol should support reliable performance using large numbers of relay nodes.

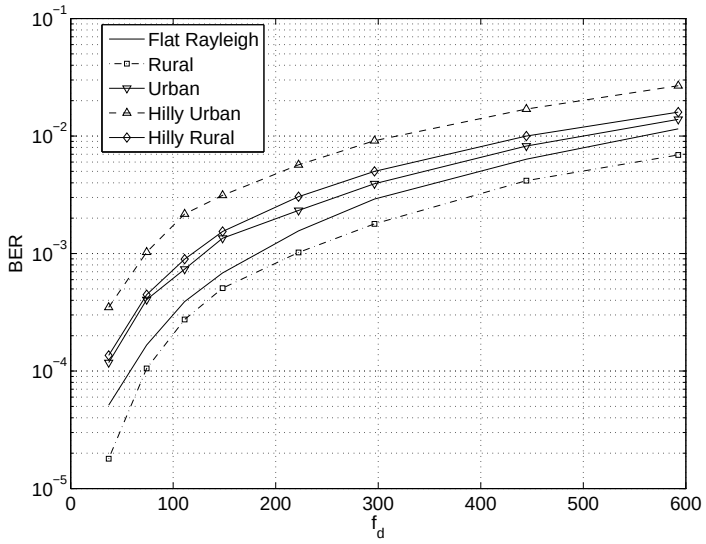

Figure 4.11: BER vs Doppler Spread for a 4 hop link with PF relays

This can be seen in Fig. 4.15 where the number of hops that can be tolerated increases from 2 at an SNR of approximately 23dB to 16 at 32dB.

4.6 Block Error Rates

This simulation is similar to the BER limit simulation, with the addition of a convolutional encoder at the original transmitter and Viterbi decoder at the final receiver. The encoding/decoding scheme used is the same as that of the DecR relaying protocol described in Sec. 4.2. The first and last links are again faded at a 100km/h effective velocity with a 800MHz carrier. The encoded blocks consist of 196 bits with the last two symbols always being zero. With a half rate code this results in 96 bits of information per block. The SNR is the same at each node so the simulation again represents a transmission distance which increases linearly with the number of hops.

Figures 4.16 and 4.17 show the results. It is interesting to note that the DecR relays do not significantly outperform the DetR relays. This could be attributed to the fact that, at this low error rate, performance is most likely dominated by a single bad link. In this situation, the decoder at the final receiver can be as effective

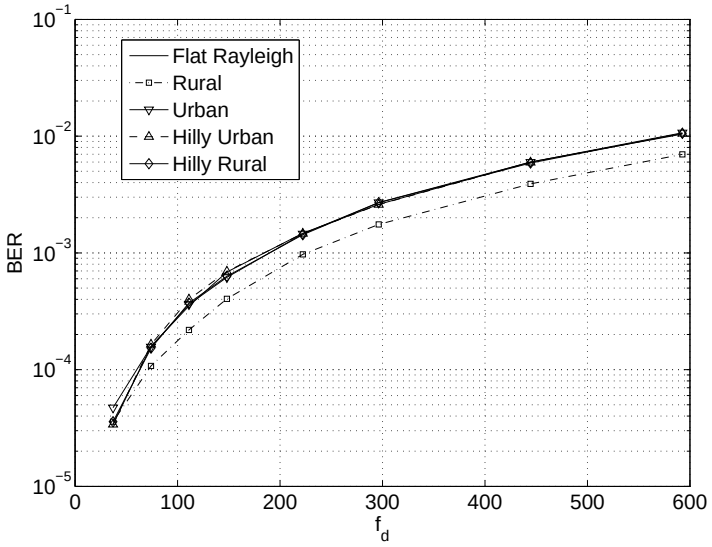

Figure 4.12: BER vs Doppler spread for a 4 hop link with DetR relays

as having a decoder in the relay receiving the weak signal. To further investigate this, we will look at the requirements for maintaining a 5% BLER, shown in Figs. 4.19 and 4.20. With PF relaying the results show similar trends to the BER results in Fig. 4.14. As is the case with transmission without FEC, the PF relays cause the effects of ISI to compound with number of hops.

At a 5% BLER the DecR and DetR protocols still provide similar results as shown in Figs. 4.19 and 4.20. This suggests that DecR relays are unnecessary for the network scenarios considered here. In order to see what advantages the FEC could provide, Figs. 4.21 and 4.22 show BER for a range of SNR values for a 4 hop relay link. We can see, when comparing to Fig. 4.8, that while the FEC provides an improvement in BER, the use of DecR relays does not significantly increase this advantage.

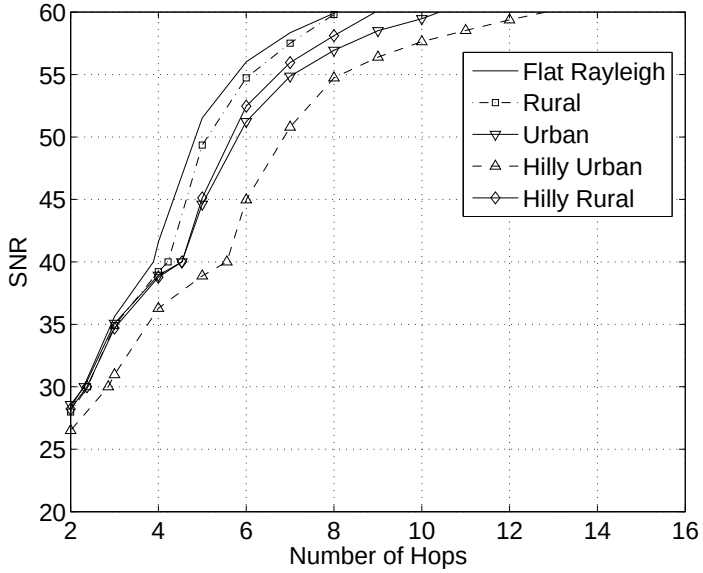

Figure 4.13: 2% BER contours for AF relays with 100km/h faded first and last links.

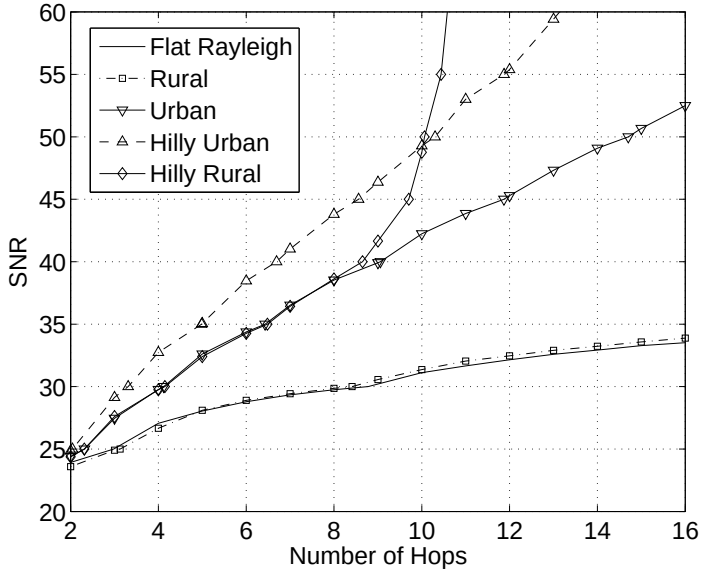

Figure 4.14: 2% BER contours for PF relays with 100km/h faded first and last links.

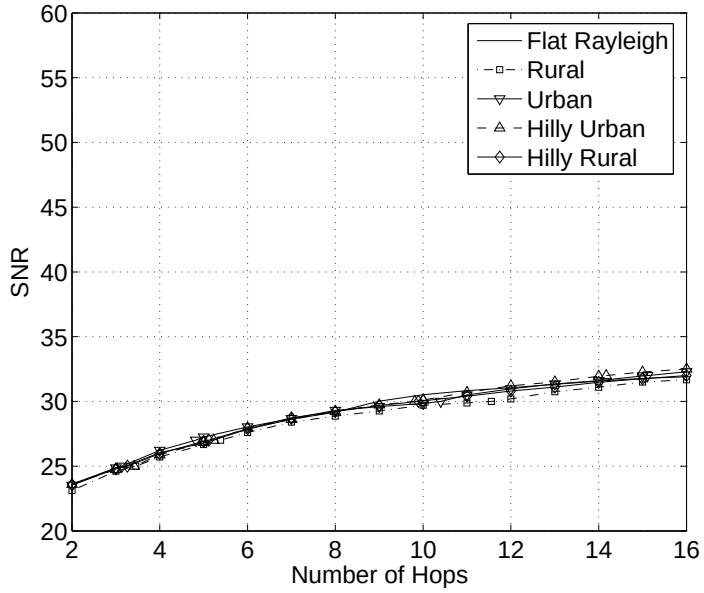

Figure 4.15: 2% BER contours for DetR relays with 100km/h faded first and last links.

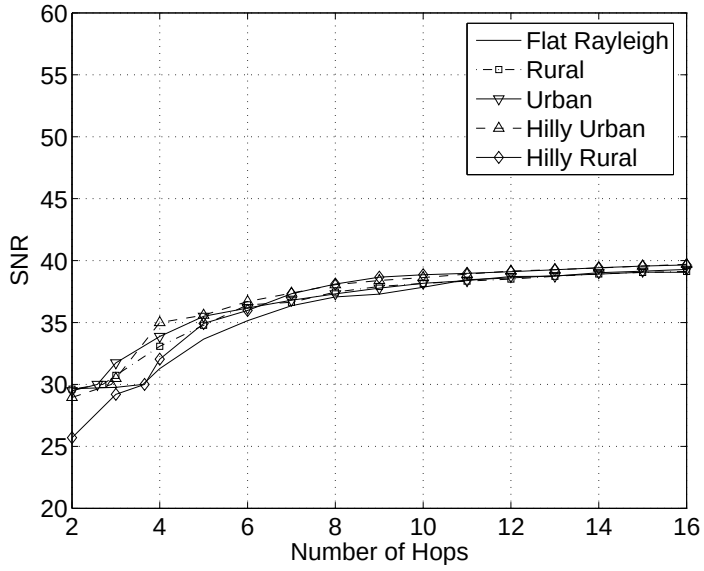

Figure 4.16: 1% block error rate contours for DecR relays with half rate coding.

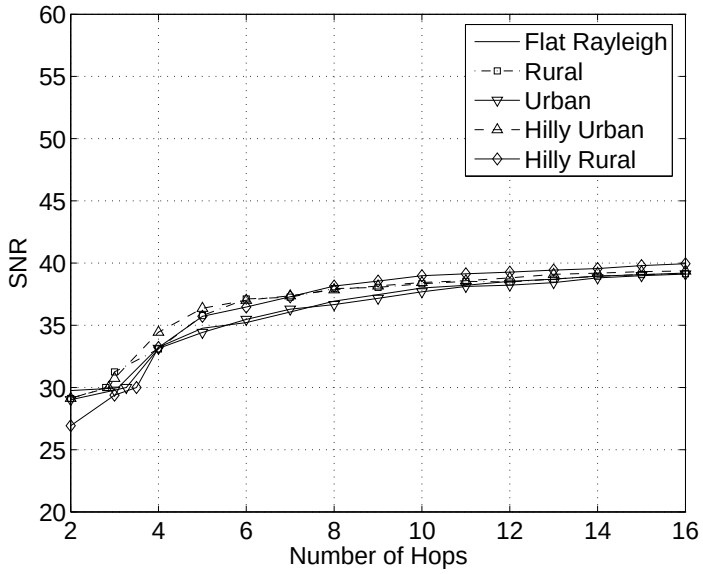

Figure 4.17: 1% block error rate contours for DetR relays with half rate coding.

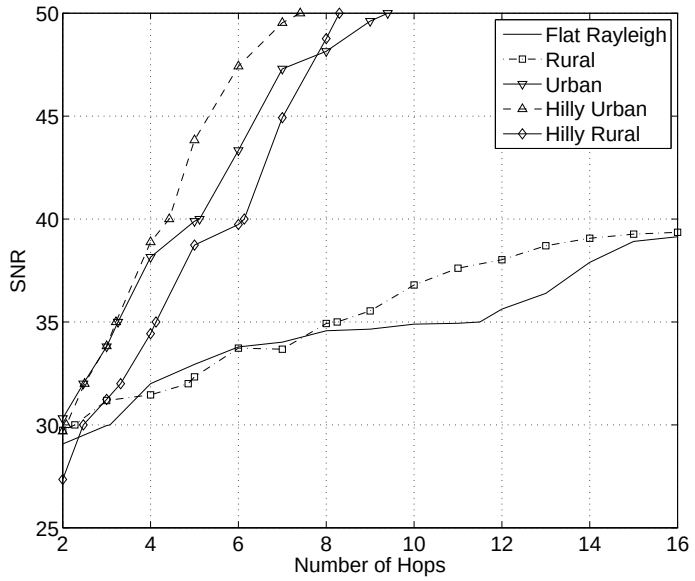

Figure 4.18: 1% block error rate contours for PF relays with half rate coding.

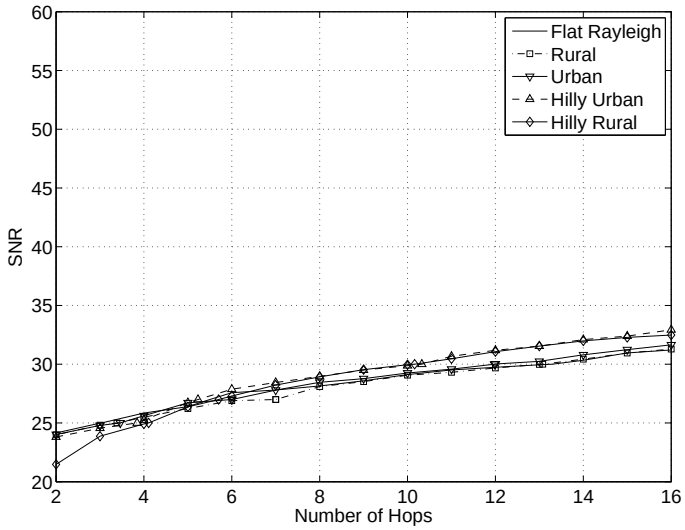

Figure 4.19: 5% block error rate contours for DecR relays with half rate coding.

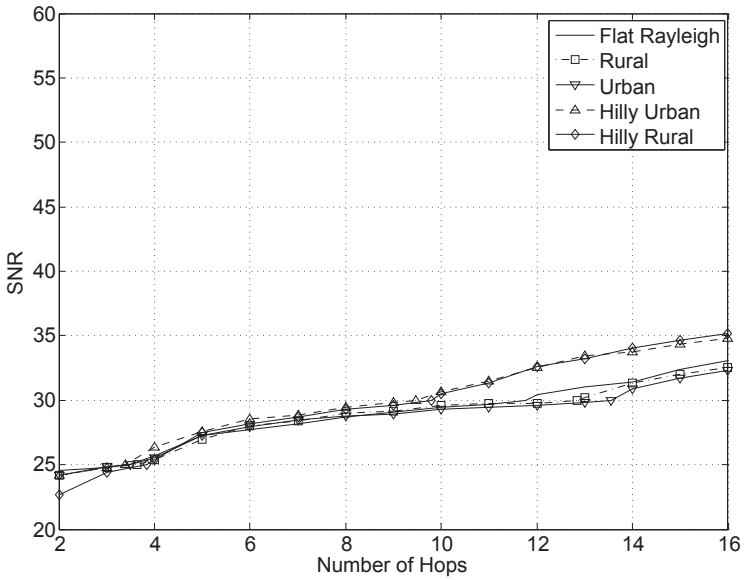

Figure 4.20: 5% block error rate contours for DetR relays with half rate coding.

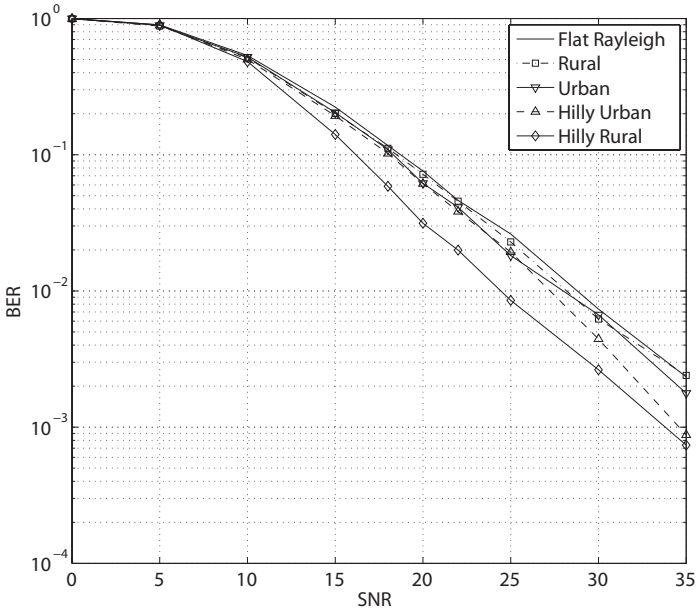

Figure 4.21: BER vs SNR for DecR relays with half rate coding.

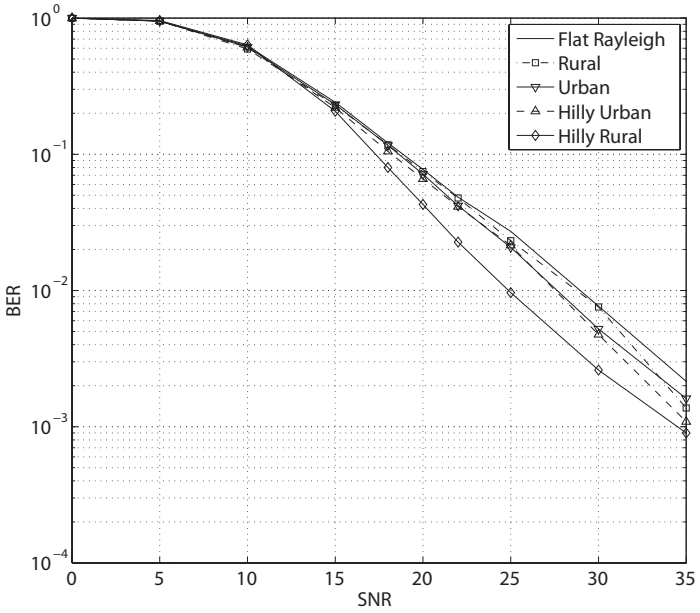

Figure 4.22: BER vs SNR for DetR relays with half rate coding.

Chapter 5

Conclusions and Future Work

In Chap. 3 we began the original work in the thesis by developing an end to end statistical model for the multi-hop MIMO relay channel. Unfortunately, a full representation of the statistics of the system has proved difficult to obtain and our end to end model is unable to simply model the dependence between the signals at separate receiver antennas. While this problem has so far proved persistent, the current model is an exact description of the statistics of the signal at a single receive antenna. This is of particular relevance to a multiple input single output system, for which it is a complete statistical model. It can also be used to explore properties of a full MIMO system. Presented in Chap. 3 are expressions for the moments of the channel statistics. Included are moments of elements of the equivalent channel matrix and noise vector. We also find an expression for the moments of the instantaneous noise to signal ratio at each receive antenna. The approach taken is applicable to all linear relaying protocols but for protocols in which the relay transfer matrix is a function of the channel properties it may not be tractable. An important case in which the relay matrices are independent of the channel is that of a fixed gain relay. For this system, we show that the expected received signal power decreases exponentially with the number of hops and the expected noise power increases as the sum of an exponentially decreasing sequence. It was found that the end to end SNR decreased exponentially with an increasing number of hops, when this number is large. The rate of this decrease drops with increasing antenna numbers. Looking at

the eigenvalues of the equivalent channel matrix establishes bounds on the recevied power of the eigenchannels. Here, we see that as the number of antennas increases, the received power of the weaker eigenchannels tends to zero while the power of the dominant eigenchannel increases. We also see that the average eigenvalue decreases showing that the full diversity gains offered by the increased antenna numbers are not being realised. Finally, we have shown that the equivalent noise term can be approximated by an independent complex Gaussian distribution, with the resulting system model providing a useful upper bound on BER.

With P25 relay chains, the most significant channel properties are the instantaneous channel gains and power delay profile. The time varying phase component of the channel has a lesser effect on BER, for the modulation rate and carrier frequencies used, at the expected relative radio node speeds. The result of multiple relay hops on each of these channel properties depends on the relaying protocol used. With amplify and forward relays, the degradation due to channel gain and ISI is compounded with increasing hops. This results in poor performance, irrespective of the radio environment. Using AF relays, the instantaneous channel gains dominate BER results. PF relays can better control the variance in channel gains over multiple hops and outperform the AF protocol in all environments. With PF relays, ISI dominates BER with increasing relay nodes, as this effect still increases with the number of hops. Phase forwarding could be appropriate in environments with low delay spreads, for example high-site networks, but is significantly outperformed by DetR relays if this is not the case. DetR relays prevent ISI from increasing with the number of hops and outperforms both AF and PF relays in all of the environments considered. For data transmission, where block error rates are a concern, the DetR and DecR results are similar across all of the environments considered. This suggests that DecR relays are unnecessary for the senarios considered.

There are numerous gaps in this analysis that warrant further investigation. Firstly, an end to end reduced statistical model that retains the dependence between the signals at the receive antennas would be desirable. It should be noted that the possibility of finding such a model does not look promising at this stage. More

fruitful directions of research may be the pursuit of BER expressions for a single output system, although obtaining such a result would still apear to be difficult. A wider range of relaying protocols need to be considered, including optimal diagonal and full linear relays. These protocols that rely on channel state information at the relays could result in much simpler models as the end to end system becomes more deterministic.

Chapter 6

Appendix

6.1 FEC Algorithms

```
%Function to perform encoding of signals using the half rate code

function y = enc_intrleave1_2(x)

InterleavingTable = [0 1 8 9 16 17 24 25 32 33 40 41....
                     48 49 56 57 64 65 72 73 80 81 88 89 96 97....
        2 3 10 11 18 19 26 27 34 35 42 43....
        50 51 58 59 66 67 74 75 82 83 90 91....
        4 5 12 13 20 21 28 29 36 37 44 45....
        52 53 60 61 68 69 76 77 84 85 92 93....
        6 7 14 15 22 23 30 31 38 39 46 47....
        54 55 62 63 70 71 78 79 86 87 94 95];

signalP = [0 2;
           2 2;
           1 3;
           3 3;
           3 2;
           1 2;
           2 3;
           0 3;
           3 1;
           1 1;
           2 0;
           0 0;
           0 1;
           2 1;
           1 0;
           3 0];

halfRateStateMachine = [ 0  15 12   3;      % [state][input]   % Remember rows are
                         4  11  8   7;      % Refer TIA/EIA 102.BAAA Table 7-2
                         13   2  1  14;     % Note: This table is used to index th
                         9   6  5  10  ];

invHalfRateLevelsConstellation = [8 3 4 15;      % This matrix has been calculated
                                  11 0 7 12;     % being used to index the constel
                                  6 13 10 1;     % 102.BAAA. The important thing t
                                  5 14 9  2];
currentState = 0;
enc_x = [];
%Encoding Loop
for encIndx = 1:length(x)
    enc_x = [enc_x signalP(halfRateStateMachine(currentState+1, x(encIndx)+1)+1, :
    currentState = x(encIndx);
end

%Interleaving Loop
for intlevIndx = 1:length(InterleavingTable)
    y(intlevIndx) = enc_x(InterleavingTable(intlevIndx)+1);
end
```

```
%Function to perform decoding of signals using the half rate code

function y = deinterleave_decode1_2(x)

InterleavingTable = [0 1 8 9 16 17 24 25 32 33 40 41....
                     48 49 56 57 64 65 72 73 80 81 88 89 96 97....
        2 3 10 11 18 19 26 27 34 35 42 43....
        50 51 58 59 66 67 74 75 82 83 90 91....
        4 5 12 13 20 21 28 29 36 37 44 45....
        52 53 60 61 68 69 76 77 84 85 92 93....
        6 7 14 15 22 23 30 31 38 39 46 47....
        54 55 62 63 70 71 78 79 86 87 94 95];

                                            %                    The New State
                                            %                     0  1  2  3
                                            %                    ----------
invHalfRateTrellis = [1  1  1  1;           %                    | 0  0  0  0
                      2  2  2  2;           %                    | 1  1  1  1    Th
                      3  3  3  3;           %                    | 2  2  2  2
                      4  4  4  4 ];         %                    | 3  3  3  3

invHalfRateLevelsConstellation = [8 3 4 15;      % This matrix has been calculated
                                  11 0 7 12;     % being used to index the constel
                                  6 13 10 1;     % 102.BAAA. The important thing t
                                  5 14 9  2];    % following symbol table applied
                                                 % this is turned around MSB<-LSB
                                                 % position 3 along and 2 down, of
                                                 % table 7-3 = symbols -3,
                                                 % +3 which is 1110 which is 7
de2biLUT = [0 0 0 0;
            1 0 0 0;
            0 1 0 0;
            1 1 0 0;
            0 0 1 0;
            1 0 1 0;
            0 1 1 0;
            1 1 1 0;
            0 0 0 1;
            1 0 0 1;
            0 1 0 1;
            1 1 0 1;
            0 0 1 1;
            1 0 1 1;
            0 1 1 1;
            1 1 1 1];

for deInterleaveIndex = 1:length(InterleavingTable)
    deintleaved_x(InterleavingTable(deInterleaveIndex)+1) = x(deInterleaveIndex);
end

encodedMessageSize = length(deintleaved_x)/2;
for indx = 1:encodedMessageSize
    x_pairs(indx) = deintleaved_x(2*indx-1) + 4*deintleaved_x(2*indx);
end

survivingPaths = [0;0;0;0];

NewSurvivingPath1 = zeros(1,encodedMessageSize);
NewSurvivingPath2 = zeros(1,encodedMessageSize);
NewSurvivingPath3 = zeros(1,encodedMessageSize);
NewSurvivingPath4 = zeros(1,encodedMessageSize);
Metrics = 100*ones(1,4);                          % The current metric for each o
Metrics(1) = 0;
```

```
for index = 1:encodedMessageSize
    x_pair = x_pairs(index);
    CompareMetrics = [];               % Clear the compare metric matrix each time
    for i = 1:4           % ROW             % For Each new state calculate the met
        for j = 1:4       % COLUMN
            hammingDistance = sum( xor( de2biLUT(invHalfRateLevelsConstellation(i,
            CompareMetrics(i,j) = Metrics(i) + hammingDistance;
        end
   end
   CompareMetrics;


  [minValue minCol] = min(CompareMetrics);     % Do the compare for each state to

   [C,D] = size(survivingPaths);

   NewSurvivingPath1 = [survivingPaths(invHalfRateTrellis(minCol(1),1),1:D) 0];
   NewSurvivingPath2 = [survivingPaths(invHalfRateTrellis(minCol(2),2),1:D) 1];
   NewSurvivingPath3 = [survivingPaths(invHalfRateTrellis(minCol(3),3),1:D) 2];
   NewSurvivingPath4 = [survivingPaths(invHalfRateTrellis(minCol(4),4),1:D) 3];

   survivingPaths = [];
   survivingPaths = [NewSurvivingPath1;NewSurvivingPath2;NewSurvivingPath3;NewSurv

   Metrics = minValue;
end

y = survivingPaths(1,1:D);
```

Published with MATLAB® 7.10

Bibliography

[1] A. Leon-Garcia and I. Widjaja, *Communications Networks: Fundamental Concepts and Key Architectures*, 2nd ed. Boston: McGraw-Hill, 2004.

[2] W. C. Y. Lee, *Wireless and Cellular Telecommunications*, 3rd ed. New York: McGraw-Hill, 2006.

[3] Standards New Zealand, *Radiocommunications Equipment used in the UHF Citizens Radio Band Radio Service*, 2nd ed. Wellington [N.Z.] : Standards New Zealand, 2002.

[4] C. H. Sterling, *The Museum of Broadcast Communications Encyclopedia of Radio.* New York : Fitzroy Dearbon, 2004.

[5] H. Carl, *Radio Relay Systems.* London: Macdonald, 1966.

[6] Anonymous, "The mobile repeater emerges," *Wireless Review*, vol. 15, p. 120, 1998.

[7] P. Delogne, *Leaky Feeders and Subsurface Radio Communication.* Stevenage, Herts. : P. Peregrinus, on behalf of the Institution of Electrical Engineers, 1982.

[8] N. Swartz, "Hybrid repeaters in the spotlight," *Wireless Review*, vol. 15, p. 40, 1998.

[9] H. L. Bertoni, *Radio Propagation for Modern Wireless Systems.* Upper Saddle River, NJ: Prentice Hall PTR, 2000.

[10] O. Oyman, N. Laneman, and S. Sandhu, "Multihop relaying for broadband wireless mesh networks: From theory to practice," *IEEE Commun. Mag.*, vol. 45, pp. 116–122, 2007.

[11] G. Kramer, R. Berry, H. El Gamal, M. Franceschetti, M. Gastpar, and J. Laneman, "Introduction to the special issue on models, theory, and codes for cooperation in communication networks," *IEEE Trans. Inf. Theory*, vol. 52, pp. 3297–3301, 2007.

[12] Y. Wang, F. Liu, S. Xu, X. Wang, Y. Qian, and P. Wang, "Performance analysis of multi-hop MIMO relay network," in *Communications Workshops, 2008. ICC Workshops '08. IEEE International Conference on*, 19-23 2008, pp. 6–10.

[13] A. Sulyman, G. Takahara, H. Hassanein, and M. Kousa, "Multi-hop capacity of MIMO-multiplexing relaying systems," *Wireless Communications, IEEE Transactions on*, vol. 8, no. 6, pp. 3095–3103, June 2009.

[14] Y. Rong and Y. Hua, "Optimality of diagonalization of multi-hop MIMO relays," *Wireless Communications, IEEE Transactions on*, vol. 8, no. 12, pp. 6068 –6077, December 2009.

[15] K. J. R. Liu, A. K. Sadek, W. Su, and A. Kwasinski, *Cooperative Communications and Networking*. New York: Cambridge University Press, 2009.

[16] J. Boyer, D. Falconer, and H. Yanikomeroglu, "A theoretical characterization of the multihop wireless communications channel with diversity," *Global Telecommunications Conference, IEEE*, pp. 841–845, Nov 2001.

[17] ——, "A theoretical characterization of the multihop wireless communications channel without diversity," *2001 IEEE International Symposium on Personal, Indoor and Mobile Comms.*, pp. E–116–E–120, Sep/Oct 2001.

[18] C. Conne, M. Ju, Z. Yi, H. Song, and I. Kim, "SER analysis and PDF derivation for multi-hop amplify-and-forward relay systems," *Communications, IEEE Transactions on*, vol. 58, no. 8, pp. 2413–2424, August 2010.

[19] I.-M. Kim, Z. Yi, M. Ju, and H.-K. Song, "Exact SNR analysis in multihop cooperative diversity networks," in *Proc. IEEE CCECE*, 2008, pp. 843–846.

[20] A. K. Sadek, W. Su, and K. J. R. Liu, "Multinode cooperative communications in wireless networks," *IEEE Trans. Signal Processing*, vol. 55, pp. 341–351, 2007.

[21] N. L. Johnson, S. Kotz, and N. Balakrishnan, *Continuous Univariate Distributions*, 2nd ed. John Wiley & Sons, 1994, vol. 1.

[22] E. Biglieri, R. Calderbank, A. Constantinides, A. Goldsmith, A. Paulraj, and H. V. Poor, *MIMO Wireless Communications*. Cambridge University Press, 2007.

[23] Luxembourg : Office for Official Publications of the European Communities, *COST 207 Digital Land Mobile Radio Communications*, 1989.

[24] T. I. Association, *Project 25 FDMA Common Air Interface*.

[25] C. S. Patel, G. L. Stuber, and T. G. Pratt, "Statistical properties of amplify and forward relay fading channels," *IEEE Trans. Veh. Technol.*, vol. 55, pp. 1–9, 2006.

[26] G. Sharma, V. Ganwani, U. Desai, and S. Merchant, "Performance analysis of maximum likelihood detection for decode and forward MIMO relay channels in Rayleigh fading," in *Wireless Communications and Networking Conference*, 2009, pp. 1–6.

[27] I. S. Gradshteyn and I. M. Ryzhik, *Table of Integrals, Series, and Products*, 4th ed. Academic Press: New York and London, 1965.